Hydro

SANDIA REPORT

SAND88—1156 • UC—70
Unlimited Release
Printed March 1989

A Review of Near Field Seawater-Sediment Interactions With Application to the Subseabed Disposal of Nuclear Waste

J. L. Krumhansl

Prepared by
Sandia National Laboratories
Albuquerque, New Mexico 87185 and Livermore, California 94550
for the United States Department of Energy
under Contract DE-AC04-76DP00789

HYDROLOGY DOCUMENT NUMBER 504

SF2900Q(8-81)

Issued by Sandia National Laboratories, operated for the United States Department of Energy by Sandia Corporation.

NOTICE: This report was prepared as an account of work sponsored by an agency of the United States Government. Neither the United States Government nor any agency thereof, nor any of their employees, nor any of their contractors, subcontractors, or their employees, makes any warranty, express or implied, or assumes any legal liability or responsibility for the accuracy, completeness, or usefulness of any information, apparatus, product, or process disclosed, or represents that its use would not infringe privately owned rights. Reference herein to any specific commercial product, process, or service by trade name, trademark, manufacturer, or otherwise, does not necessarily constitute or imply its endorsement, recommendation, or favoring by the United States Government, any agency thereof or any of their contractors or subcontractors. The views and opinions expressed herein do not necessarily state or reflect those of the United States Government, any agency thereof or any of their contractors or subcontractors.

Printed in the United States of America. This report has been reproduced directly from the best available copy.

Available to DOE and DOE contractors from
Office of Scientific and Technical Information
PO Box 62
Oak Ridge, TN 37831

Prices available from (615) 576-8401, FTS 626-8401

Available to the public from
National Technical Information Service
US Department of Commerce
5285 Port Royal Rd
Springfield, VA 22161

NTIS price codes
Printed copy: A04
Microfiche copy: A01

Distribution
Category UC-70

SAND88-1156
Unlimited Release
Printed

A REVIEW OF NEAR FIELD SEAWATER-SEDIMENT INTERACTIONS WITH APPLICATION TO THE SUBSEABED DISPOSAL OF NUCLEAR WASTE

J.L. Krumhansl
Division 6233
Sandia National Laboratories

March 10, 1989

This Page Intentionally Left Blank

ABSTRACT

Disposal of spent fuel or high level nuclear waste into marine sediments would create high temperature - high gamma radiation environments adjacent to waste canisters. Under these conditions sediments will react producing pore waters that differ significantly from those occurring naturally. These changes may enhance canister corrosion or facilitate transport of radionuclides through unreacted sediments beyond the heated zone. In addition, the term "near field" needs clarification as it is used widely without having a precise meaning. Research in three areas was undertaken to improve our understanding of near field chemical processes. Initially, isothermal experiments were carried out in "Dickson" hydrothermal systems. These were followed by an experimental program directed at understanding the chemical effects of temperature-gradient induced transport. Finally, additional experimentation was done to study the combined effects of hydrothermal conditions and intense gamma radiation. Having completed this body of experimental work, it was concluded that near field conditions are not an obstacle to the safe use of abyssal marine sediments for the disposal of spent fuel or high level nuclear wastes.

Isothermal experiments were done with a variety of sediments. With clay rich sediments an acidic condition developed. At 200°C, the pH generally remained above 4 while at 300°C, transient pH values below 3 were noted. The underlying mechanism responsible for this is the combination of silica (from the sediment) with water and magnesium (from the seawater) to produce a talc component in the clay, along with hydrogen ions. In organic rich sediments pyrolysis may also contribute to the acidification process. Both acetic and formic acids have been identified in fluid samples from such experiments. Trace element mobility was also monitored in all experiments. In general, significant fractions of the B, Pb, Cu, and Zn in the sediment were mobilized, while Ni, Cr, Co, Ba, and Sr were relatively immobile. Significant dissolved Fe and Mn concentrations were also noted with the Fe to Mn ratio being definitively higher in strongly reducing solutions.

Placing sediments in a temperature gradient revealed that both convection and transport in response to the Soret effect ("Soret transport") could have a profound effect on near field chemistry. Soret transport, in general, caused the major solutes of seawater to leave the hottest, most reactive part of an experiment. This process will eventually reach an equilibrium condition where further transport ceases. The quantitative application of this principle to actual sediments is, however, greatly complicated by the large number of sources and sinks that arise as hydrothermal seawater-sediment interactions add or subtract components to or from the solution. In contrast to Soret transport, convection has the potential for delivering a continuous supply of reactive components to the hottest part of an experimental system. In the ISIMU experiment, active convection dominated the region nearest the heater. The net effect was a sediment depleted in quartz, illite and kaolinite. At the same time, the sediment had become enriched in K-feldspar, Mg-rich chlorite and analcime. Analcime, in particular, owed its origin to the continual supply of seawater supplied by convection. This kept the pH relatively high, maintained an elevated sodium concentration, and at the same time flushed the dissolved silica out quickly enough that fluids remained undersaturated

with respect to quartz. Beyond the (hottest) zone where seawater actively circulated, Soret transport resulted in a concentric zone enriched in quartz and chlorite.

When radiation was finally added to the experimental matrix no mineralogic changes were detectable that had not already been observed in radiation-free experiments. Gaseous radiolysis products, however, were found. The ratio of radiolytic hydrogen to radiolytic oxygen typically exceeded the ideal value of two. Two would be expected if the breakdown of water was the only process occurring in the experiment. It is likely that the missing oxygen was consumed by oxidizing organic matter to form carbon dioxide or organic acids. It was also found that the G values for the production of radiolytic hydrogen gas were below the value observed in deionized water. Thus, the G value in deionized water (0.45) would provide a conservative over estimate for use in mass balance calculations. Finally, when the combined effects of temperature and radiation gradients were evaluated, no new phenomena were observed.

The results of this study have a number of programmatic applications. A variety of pH values must be considered ranging from essentially neutral to mildly acidic. However, a pH of 3 is a useful lower limit. In the same experiments it was established that conditions may vary from mildly oxidizing to strongly reducing. Mineralogic reactions were also found that permanently alter the nature of the sediment, and thus serve to characterize the near field. These changes, however, require temperatures above 50°C. Thus, the maximum extent of the 50°C isotherm provides a convenient outer boundary for the near field. With regard to radiation effects, the most common radiolysis products were oxygen and hydrogen gas. It is unlikely that enough gas could be generated, though, to embrittle a titanium canister or form bubbles adjacent to it. All of the experiments in this study were performed in autoclaves using titanium components. As corrosion was never observed, it seems reasonable to suggest that titanium would make a suitable canister material. To conclude, a detailed history of the chemical evolution of the near field is still not possible. This follows because the rates of the important reactions as identified in this study remain unknown. The present data base is, however, sufficient to confirm that near field chemical reactions are not a major stumbling block to the subseabed disposal of spent fuel or nuclear waste.

TABLE OF CONTENTS

ABSTRACT 5
TABLE OF CONTENTS 7
INTRODUCTION 9
1.0 ISOTHERMAL EXPERIMENTS 9
Table 1 17
Table 2 22
2.0 EXPERIMENTS IN A TEMPERATURE GRADIENT 23
2.1 Soret Transport 23
Table 3 26
Table 4 27
Table 5 28
2.2 Combined Convection and Soret Transport 31
Table 6 33
3.0 RADIATION EFFECTS IN THE NEAR FIELD 35
3.1 Isothermal Seawater-Sediment-Radiation Interactions Studies 35
Table 7 36
3.1.1 Mineralogy and Solution Chemistry 37
Table 8 38
3.1.2 Radiolysis Effects 39
Table 9 40
Table 10 41
Table 11 41
3.2 Synergistic Effects Involving Radiation and Temperature Gradients 42
3.2.1 Mineralogic and Textural Observations 42
3.2.2 Transport Processes and Inorganic Solution Chemistry 43
3.2.3 Organic Chemistry 46
3.2.4 Radiation Effects 46
Table 12 47
Table 13A 47
Table 13B 48
Table 14 49
Table 15 50
Table 16 50
Table 17 50
4.0 PROGRAMMATIC APPLICATIONS 52
REFERENCES 55
FIGURES 59

This Page Intentionally Left Blank

INTRODUCTION

The "near field" is that region exposed to elevated temperatures and gamma radiation which lies between a waste canister and sediments in their "natural" condition. Neither marine minerals nor pore fluids can resist change in such an anomalous environment. The near field is also a relatively small region. Sediments beyond approximately 0.8 meter from a canister will never receive a significant radiation dose or experience temperatures above 100°C; while those lying further than 1.7 meters will not even reach 50°C. Consequently, the near field may also be characterized as a region where strong gradients exist. Because of this, coupled heat and mass transfer processes will aeffect how the sediment equilibrates to its new environment. Research on this complex region is justifiable in terms of the following programmatic objectives:

(1) Current waste management strategy holds that canisters must last for several centuries. To accomplish this, it is necessary to understand the hydrothermal environment that will persist during the first several decades following emplacement.

(2) It is also necessary to establish that near field effects will not short circuit the barrier provided by far field sediments.

(3) Though the term "near field" is widely used (sometimes in a regulatory sense), it has no legitimate usage until the time frame is stated, specific chemical changes responsible for displacing sediments from their "natural" condition are identified, and some perspective is gained regarding the conditions under which these processes operate effectively.

A three stage approach was used to address these matters. Initially, isothermal experiments were carried out on a variety of sediment types to isolate the dominant chemical reactions occurring at various temperatures (Part 1). The next level of activity involved considering the coupled effects of sediment-water interactions and thermally driven transport processes (Part 2). The last phase of the investigation was directed at incorporating the influence of gamma radiation into the experimental matrix (Part 3).

1.0 ISOTHERMAL EXPERIMENTS

The study of hydrothermal reactions under isothermal conditions has benefited greatly from the development of the "Dickson" hydrothermal apparatus (1). Briefly, the system consists of an autoclave able to sustain pressures of 50 MPa at 300°C, an internal liner, and a rocking furnace so that the solids are kept suspended in the reacting fluid while the entire assembly is heated. The liner consists of a thin flexible gold or titanium bag that attaches to a titanium head. This, in turn, connects to an external sample valve. Pressure is maintained by pumping water into the space outside the bag. Consequently, sequential samples may be withdrawn during the course of a reaction without changing the run pressure or adding fresh fluid to the reaction chamber. After its development in the early 1970's, one of the first applications was a study of seawater

chemistry to 350°C (2,3). Although seawater is mildly basic at room temperature, heating to 250°C causes a slight drop in quench pH from around 7.7 to 5.8. Bischoff and Seyfried (2) attributed this change to oxidation of a small amount of dissolved organic material in the seawater. The only precipitation reaction noted over this interval was that of anhydrite, which initially reached saturation slightly above 150°C and remained saturated to 350°C This, however, had a minimal effect on solution pH since the sulfate-bisulfate buffer is not important at low temperatures. Above 250°C, the appearance of a new phase, magnesium hydroxysulfate, greatly increases the amount of acid produced. The generalized reaction can be characterized as (3):

$$(n+1)Mg^{++} + SO_4^{=} + H_2O \text{ ---> } (2n)H^+ = (n)Mg(OH)_2.MgSO_4.(1-2n)H_2O. \qquad \text{(Eq. 1.1)}$$

At 300°C, this reaction proceeds so vigorously that a quench pH of 3.0 results.

Adding marine sediments to heated seawater greatly complicates the picture (Table 1). Many more reactions are possible, and most of the important reactions require years to reach equilibrium (4,5,6,7,8). None the less, seawater-sediment systems share one important characteristic with seawater alone: they generally produce mildly acidic fluids at high temperatures. To investigate the behavior of such systems several different sediment types were mixed with seawater in a ratio of 1 to 5*, and then reacted in Dickson hydrothermal systems. The sediment to be discussed first is a relatively organic rich (Table 2) gray-green silty clay ("V36") from the western North Pacific (4,7,8,). One difference noted immediately (Table 1, entry #1) was that, in contrast to the behavior of seawater alone, these fluids actually became undersaturated with respect to magnesium hydroxysulfate within a few hours after reaching 300°C. However, both acid production and magnesium consumption continued throughout the experiment. When the experiment was finished, the sediment was found to be poorer in silica-rich amorphous material, organic carbon and plagioclase. Smectite, however, was more abundant and the sediment was somewhat enriched in magnesium. (Illite and chlorite appeared little affected.) In simplified form the principal reaction responsible for these changes is:

$$3Mg^{++} + 4SiO_2 + 4H_2O \text{ ---> } Mg_3Si_4O_{10}(OH)_2 + 6H^+. \qquad \text{(Eq. 1.2)}$$

Whether discrete talc layers actually exist is questionable, but formation of a smectite-like phyllosilicate with a preponderance of its octahedral sites occupied by magnesium has been verified by this author using an analytic transmission electron microscope.

*This ratio was necessitated by the desire to help the mixture fluid so that the gentle rocking motion imparted to the autoclave could stir it, and by the constraint that an experiment contain enough fluid so that a number of sequential samples could be taken. Normal marine sediments have a significantly higher sediment to seawater ratio. As a consequence, in these experiments reactions liberating or consuming components to or from seawater respectively should have gone further than in the natural setting, provided the natural sediments behave as essentially closed systems.

A second aspect of heating this particular sediment is the effect of temperature on the organic material. Although no analyses were performed for organic acids they undoubtedly formed (9, 10), and probably contributed to the initially low pH. Likely candidates are formic and acetic acids, the formation of which can be grossly represented by:

$$nCH_2O \text{ ----> } (n-2)CH_2O + CH_3COO^- + H^+ \text{ and} \qquad \text{(Eq. 1.3)}$$

$$0.5O_2 + CH_2O \text{ ---> } COOH^- + H^+. \qquad \text{(Eq. 1.4)}$$

These acids are, in turn, susceptible to further breakdown by decarboxylation reactions (11,12) - producing carbon dioxide and hydrogen or methane, and additional oxidation - producing water and carbon dioxide. Thus, once formed one might anticipate that their slow destruction would cause the pH to rise gradually, as indeed was observed. Even without the loss of organic acids, however, the pH would slowly rebound due to the hydrolysis of silicate minerals. Evidence for such a process can be found in the fact that the slow rise in pH is coupled with increases in K, Na, and Ca (from dissolution of feldspar, and in the case of K from illite dissolution as well). Calcium from this process accounts for the decreasing sulfate since anhydrite would precipitate on addition of calcium to a solution already saturated with respect to calcium sulfate. Additional silica was also provided by these processes, thus allowing for the continued removal of magnesium from solution due to saponitic smectite production.

Although dramatic changes occurred at 300°C, such changes would be confined to the hottest region immediately adjacent to a waste canister. At 200°C magnesium hydroxysulfate fails to form so acidic conditions could only arise from production of organic acids or magnesium-rich clays. Both pH and magnesium did, in fact, fall during a V36 experiments at 200°C, but only about a tenth as much hydrogen ion was produced as at 300°C. Interactions involving organic materials also appear to be much attenuated. A sensitive indicator of the pyrolysis of organic matter is the extent to which reduced iron and manganese dissolve. Since manganese in solution at 200°C was only about 60% of that at 300°C and iron was significantly less, (just a 5th of the 300° experiment), it is reasonable to suppose that the pyrolysis of the organic material also proceeded less vigorously at 200°C than at 300°C.

Only limited data are available regarding the behavior of V36 below 200°, though the general literature on pore water chemistry provides some additional guidance. The data specific to V36 comes from the early part of a temperature gradient experiment (4,13) to be described in greater detail in Part 2 of this report. A significant influx of components from the hot end of the autoclave after only 21 hours is unlikely, so the first sample from the cool end can be treated as having come from an essentially closed system. In spite of the low temperature (100°C) and short elapsed time, definite changes in fluid chemistry were noted (Table 3, Entry 2). Potassium increased by 57% (to 628 ppm), boron by 48% (to 6.5 ppm), calcium by 4% (to 427 ppm), sodium by 3% (to 11.05 ppt), while magnesium fell by 5% (to 1,237 ppm). In addition, the pH fell to 6.02 and elevated concentrations of Mn (19 ppm) and silica (250 ppm) were observed. The

elevated manganese and hydrogen ion concentration can readily be ascribed to the influence of heated organic matter, while silica polymorphs are known to be more soluble at higher temperatures. The large changes in the other solutes are, however, perplexing since new silicate minerals could not have formed in less than a day at 100°C. The resolution to this problem lies in considering the ion exchange properties of the sediment. It has been noted that even moving sediments from the seabed (about 4°C) to shipboard conditions (about 22°C) significantly shifts the balance between exchanged cations (on the clays) and pore fluid solutes (14). The general degree of reactivity is similar to what was observed with the V36 sediment at 100°C. Boron and potassium generally show the largest relative increase (by as much as 61 and 24% respectively [14]), while magnesium exhibits the greatest decrease (falling by about 7%). Only slight increases in sodium are observed, while strontium and calcium fall by variable amounts. Thus, the changes noted in V36 at 100°C probably arise from ion exchange reactions. Artificially introduced exchangeable trace elements also exhibit large and variable responses to temperature changes. For one calcareous marl studied (15), it was found that plutonium and cadmium sorption had a strong inverse correlation with temperature from 4 to 80°C, while europium and americium were little affected. Thus, whereas near field mineralogic changes probably extend to roughly the 125°C isotherm (a distance of about 0.5 meter from the canister), sediments in their "natural" state with regard to their pore fluid chemistry and sorptive properties may not be found until essentially unheated sediments are encountered (6 to 10 meters from the canister).

So far the discussion has dealt primarily with V36, an organic-rich silty clay. It is, however, equally possible that other sediment types may be used for subseabed waste disposal. The most extreme change in sediment chemistry would be the transition to a calcareous ooze. The most obvious difference (Table 1, Entry 2) is the ability of this material to neutralize any acid generated. In fact, the pH never fell much below neutrality at 300°C (2, Fig. 2), though magnesium was all but removed from solution. Silica also failed to reach the high levels noted with V36, and instead, remained at about quartz saturation. Thermodynamic modeling (employing the code SOLVEQ, Ref. 7) indicates that these solutions were approximately saturated with respect to both calcite and dolomite, but were greatly supersaturated with respect to talc (5). Thus, precipitation of a magnesium silicate had evidently not reached completion. Instead, the missing magnesium was probably incorporated into dolomite or magnesian calcite. Trace elements in solution were typically much lower than with V36, presumably in response to the higher pH and the lower content of metalliferous (Pb, Cu, Zn, Mn, Fe) and argillaceous (B) source materials in the sediment.

Other important distinctions became apparent in comparing V36 with other argillaceous sediments, some of which contain a higher proportion of smectite clays, Mn-Fe hydrous oxides, biogenic silica, or a more oxidized phase - e.g. red clays (Table 1, Entries 3-7). In large measure the observed differences in fluid chemistries reflect these features, rather than gross differences occurring in the major clay-water interactions. For example, argillaceous sediment containing a small amount of biogenic silica or volcanic glass (SM2 and V36) typically produced magnesium-rich

smectite and acid when heated. Sediments that failed to establish high silica concentrations on heating (Sediment B) also became acidic, but in this case chlorite formed rather than smectite. The conversion of indigenous smectite to illite is also favored in such settings (4,8). Hence, it is not surprising that the potassium concentrations over Sediment B were generally lower and declined more rapidly than when solutions were in contact with either V36 or SM2. One may generalize further by noting that silica concentrations above the level set by quartz saturation are temporary. With time quartz precipitation is inevitable so even sediments such as SM2 and V36 may eventually react to form the mineral assemblage: quartz + chlorite + illite (8). Whether this reaction is fast enough to proceed in the geologically short time frame relevant to waste disposal, however, has yet to be determined.

The rate at which pH rebounds also shows an obvious relationship to the trace mineral content of the sediment. The highly oxidized red clay, SM2, contains a small amount of clinoptilolite. This mineral has the typical open zeolite crystal structure and reacts more rapidly than feldspar or illite to neutralize acidity. Consequently, the pH rebounded more rapidly for SM2 than for Sediment B or V36. A second consideration is the low (Corg<.01%) organic carbon content of the highly oxidized red clays. With such materials, it is not possible to produce significant amounts of organic acids, hence their breakdown cannot influence the time required for the pH to rebound from its early minimum .

Given the experimental conditions, it is not surprising that trace elements from the sediments were dissolved. The systematics governing this mobility are, however, very complex. For example, except in the case of carbonate oozes, barium and strontium mobilities varied little with sediment type, while most other trace elements showed a much more diverse behavior. By comparing the 300°C data for V36 with Sediment B. (or with SM2 where Sediment B data is lacking) it is apparent that oxidizing conditions favor higher concentrations of Pb, Cu, Ni, Cr, and Co in solution, as well as removal of a greater proportion of these elements from the sediment. Zinc and boron concentrations were also typically higher with oxidizing sediments, but the proportion dissolved is only slightly greater for the oxidized red clays. Further examination of the proportions of metals mobilized reveals that there are two general groupings that hold for all sediment types. On one hand are those trace elements where most or all of the metal initially present in the sediment dissolves. (Compare concentrations in solution - Table 1, with the amount initially in the sediment from -Table 2, keeping in mind the experiments combined seawater and sediment in a 5:1 mixture.) Most of the boron is removed at 300°C under both oxidizing and reducing conditions. Under oxidizing conditions most of the copper is also dissolved along with roughly half the lead and zinc. Zinc and copper concentrations increased continuously during the experiment, while lead peaked at about 10 days and then fell. Under reducing conditions, slightly less than half the copper and zinc dissolved and only about 20% of the lead. Lead and zinc tended to remain in solution while this time copper decreased (though it is uncertain whether it was resorbed onto the sediment or alloyed with the gold bag). In spite of this variability, these elements all behaved in a manner that is grossly different from that of Ni, Cr, Co, Ba, and Sr. For this later group, even at peak concentration less than 1% of the metal present in the sediment

dissolved. A final important generalization regarding trace element mobility is that, except for boron, trace element mobility was sharply lower at 200°C than at 300°C.

At present, only qualitative arguments may be advanced to explain the different trace element mobilities. Boron is typically sorbed onto clays by an ion exchange process (16) and it has been demonstrated that slight shifts in pH are sufficient to effect almost complete removal. Consequently, the almost quantitative removal of boron from the sediment is consistent with the lower pH. In the case of Ba and Sr the ion products of the metal and sulfate are relatively constant, which suggests that barite and celestite solubilities may be the controlling factors. However, thermochemical modeling indicates one to two orders of magnitude undersaturation with respect to these minerals. Either the thermochemical data base on which these comparisons are based is in error, or some process such as coprecipitation with calcium in anhydrite governs their mobility. The elements typically associated with Fe-Mn oxide crusts are also problematical. In unheated sediment, it is likely that Ni and Cu both substitute for divalent manganese in the todorokite structure, while lead and cobalt are thought to substitue for tetravalent manganese in birnessite (17). Trivalent chromium can obviously substitute for iron. Further, a variety of less specific ion exchange reactions may also contribute to the trace element content of these materials. On heating, several changes occur that are likely to mobilize trace elements. High hydrogen ion concentrations may displace sorbed cations as well as dissolve a limited amount of the oxide coatings, particularly if this occurs under reducing conditions. The temperature rise also initiates transformations to the more stable (closed) hematite and pyrolusite structures. This recrystallization, in turn, excludes trace metals which then appear in solution. With so many factors tending to mobilize trace elements the question really becomes one of explaining why there are such great differences in the proportions of various elements found in solution. In the case of Cr the low mobility can be rationalized by noting that the hydroxide is extremely insoluble in even mildly acidic solutions. However, the solubilities of Ni or Co hydroxide are not much different from those of Cu, Zn, Pb, or divalent Fe and Mn hydroxide (18). Consequently, precipitation of a separate phase fails to account for the missing Co and Ni. In this case, one must go somewhat further and note that a parallel process operating in these solutions is the crystallization of the clay component. At room temperature, it has been found that most transition metals can readily proxy for magnesium during formation of sheet silicates (19), and the author has observed that this holds to at least 250°C in the case of Ni. Consequently, the missing Ni, Co, and possibly some zinc as well, are probably scavenged during formation of new smectite. On the other hand, Cu and Pb are typically excluded from silicate lattices. In nature these elements usually end up in the aqueous phase or precipitated as sulfides. With lead an additional possibility is that of forming the relatively insoluble sulfate. Thus, like strontium and barium, it too may be removed from solution as a trace component in anhydrite. Finally, one might speculate about the generally lower trace element mobilities observed at 200°C. In most part, this probably reflects the small amount of acid generated at this temperature and less vigorous reduction by the organic component in the sediments. To summarize, a number of processes limited trace element mobility in these experiments. If a trace element forms its

own insoluble hydroxide or can readily substitute for either magnesium in smectite or calcium in anhydrite then the mobility will be low even in the mildly acidic hydrothermal solutions.

Unlike the other elements that are dissolved in trace amounts, the mobilities of iron and manganese can be explained in a relatively satisfying manner. V36 is noteworthy in that its pore waters contain more iron than the other sediments while the Mn/Fe ratio in the sediment is much lower. The explanation for this lies in: (1) neither iron nor manganese can reach concentrations of several ppm in solution unless reduced to the divalent state, and (2) manganese is more readily reduced than is iron. Organic material is the most important reducing agent in these experiments, though tetravalent manganese may also be reduced by divalent iron. For V36, the solution composition reflects the fact that the sediment contains enough organic matter to reduce most of the iron as well as the manganese. With limited organic material or more manganese the situation can be reversed, e.g., SM2. Essentially, no iron is reduced or goes into solution because the manganese oxides consume the available organic matter. The net effect is a very low iron concentration and a high Mn/Fe ratio. The relative oxidation potential in these systems is also reflected in the amount of gold that dissolves from the bag; a few tenths of a part per million for V36 and several ppm for the red clays. This, in turn, has led to attempts to quantify the oxygen fugacity by the reaction:

$$Au + 2Cl^- + H^+ + 0.25O_2 \text{ ----> } AuCl_2^- + 0.5H_2O. \qquad \text{(Eq. 1.5)}$$

For the red clays oxygen fugacities in the range of 10^{-8} to 10^{-14} were obtained at 200°, and a much wider range, 10^{-6} - 10^{-20} was calculated at 300°C. V36 had a calculated oxygen fugacity value of about 10^{-20} at 300°C. However, as the above equation indicates, this estimate is predicated on an accurate knowledge of in situ pH, and on the assumption that all gold in solution exists as the complex $AuCl_2^-$. Given the high organic carbon content of the V36 sediment, (and the possibility that some of the gold in solution may have existed as an organic complex rather than $AuCl_2^-$) it seems reasonable to question the accuracy of the V36 oxygen fugacity estimate.

To summarize, isothermal studies at 200 and 300°C reveal several important processes that will affect the sediment surrounding a waste canister. In the hottest region, formation of magnesium-rich sheet silicates have a profound effect on both solution pH and Mg content, as well as considerably changing the composition of the bulk sediment. If silica levels approach those of amorphous silica saturation, then smectite may form while SiO_2 levels close to quartz saturation appear to favor chlorite-group minerals (along with illite and quartz). In addition to mobilizing a host of trace elements, a low pH may result in the dissolution of carbonate minerals along with small amounts of other silicates such as illite, zeolite and feldspars. Another important factor seems to be the pyrolysis of organic matter. In addition to reducing iron and manganese, it is likely this process lowers solution pH and provides ligands responsible for the complexing of trace elements (21). A less dramatic but nonetheless common occurrence is anhydrite precipitation. As with the reconstruction of silicate mineral this may cement individual mineral grains together, thus altering the physical properties of strongly heated sediments. Anhydrite precipitation also provides still another phase into

which trace elements may be incorporated. Finally, as the temperatures falls to around 100°C, the influence of mineralogic changes wanes, and ion exchange processes become dominant. These changes, however, are less likely to have a permanent effect on the clay. Such sediments would probably return to essentially their "natural" state once the temperature returns to normal and they are reequilibrated with the appropriate (e.g. indigenous) pore fluids.

TABLE 1

Solution Compositions during Isothermal Sediment-Seawater Interaction Experiments using Dickson Hydrothermal Systems

---

#1 V36 200°C

Non-calcareous, olive-gray, silty clay composed of quartz, plagioclase, illite, Fe-chlorite, and amorphous silica (radiolarians, diatoms, and volcanic glass) VEMA cruse 36, leg 12, 1025 - 1174 cm in core V36/12-43P, 33 deg.-45 min. N, 151 deg.-46 min. E.

Sample/hr	pH	C iorg	Na	K	Ca	Mg	SiO_2	SO_4	Cl
1/1.0	4.85	3.06	10909	539	271	1150	498	2325	19466
2/104	4.01	6.17	11194	684	172	1043	875	2412	19813
3/335	3.90	6.18	10963	703	181	967	904	2019	19907
4/669	3.79	6.41	11115	718	160	956	935	1848	19673
5/1442	3.80	6.42	10986	705	180	891	953	1709	19444
6/2254	3.70	8.22	10812	676	189	859	912	1495	19185
Q/2261	5.5	----	-----	531	462	836	554	2198	18262

	Fe	Mn	Zn	Cu	Pb	Ni	Cr	Co	Ba	Sr	Al	B	Au	Ti
1	5.5	19.6	0.9	1.7	----	----	----	0.01	0.23	3.4	0.34	5.5	<.03	0.01
2	12	48.9	1.0	0.45	----	----	----	0.01	0.23	2.0	0.14	7.1	0.06	0.01
3	17	55.5	1.0	0.56	----	----	----	<.01	0.16	1.9	0.14	7.7	0.14	0.01
4	23	61.9	1.3	0.42	----	----	----	<.01	0.28	1.8	0.18	7.8	0.12	0.01
5	36	61.8	---	0.39	----	----	----	----	0.10	2.6	0.16	8.2	0.12	----
6	34	65.4	1.4	0.27	----	----	----	----	0.11	2.7	0.16	9.2	0.04	----
Q	28	56.5	<.5	0.01	----	----	----	----	0.17	5.8	0.18	7.6	<.05	----

V36 300°C

Sample/hr	pH	C iorg	Na	K	Ca	Mg	SiO_2	SO_4	Cl
1/10	2.44	5.32	11060	649	63.8	954	1101	1734	19560
2/93.5	2.49	8.15	10928	798	98.3	529	1790	770	19353
3/284	2.72	9.68	10972	858	117	403	1819	456	19422
4/596	2.88	8.58	11082	887	136	347	1775	379	19515
5/1297	2.85	8.21	10905	921	191	290	1803	260	19277
Q/1608	4.52	1.13	-----	---	---	---	----	842	-----

	Fe	Mn	Zn	Cu	Pb	Ni	Cr	Co	Ba	Sr	Al	B	Au	Ti
1	30.3	36.3	1.7	2.8	0.66	----	----	----	0.09	1.1	0.23	7.6	<.1	----
2	181	86.5	6.8	8.4	0.97	----	----	----	0.16	0.8	0.14	9.5	0.20	----
3	231	99.7	8.5	9.4	1.10	----	----	----	0.22	1.0	0.12	9.1	0.24	----
4	229	103	8.0	7.4	1.09	----	----	----	0.28	1.0	0.12	9.0	0.24	----
5	218	108	9.1	3.3	----	----	----	----	0.37	1.4	0.13	9.4	0.24	----
Q	----	----	6.8	1.5	----	----	----	----	0.28	3.5	0.28	8.4	0.22	----

#2 Carbonate Ooze 300°C

Sample/hr	pH	C iorg	Na	K	Ca	Mg	SiO_2	SO_4	Cl
1/5.75	4.82	19.2	9835	469	73.3	964	5.4	163	18386
2/174	4.50	43.7	10340	542	1143	146	516	<150	18892
3/777	4.90	54.6	10566	775	1453	8.1	754	<150	19515
Q/846.6	5.4	59.3	11571	768	2209	34.6	429	1484	19422

	Fe	Mn	Zn	Cu	Pb	Ni	Cr	Co	Ba	Sr	Al	B	Au	Ti
1	0.76	2.09	0.65	----	0.40	----	0.05	0.01	----	3.67	0.08	----	----	----
2	1.68	3.08	0.86	----	0.36	----	0.05	----	----	64.8	----	----	----	----
3	1.59	2.59	0.68	----	0.40	----	<.01	0.03	----	64.3	0.39	----	----	----
Q	1.49	3.57	0.39	----	0.53	----	0.07	0.03	0.17	76.2	----	10.2	----	----

#3 SM2 200°C

Dark brown, smectite-rich clay, clinoptilolite, quartz, fish debris, iron oxide crusts, amorphous material (silica, ferromanganese oxyhydroxides), from GPC-2 30° -20.9 min. N., 157° -50.85 min. W (pacific smectite)

Sample/hr	pH	C iorg	Na	K	Ca	Mg	SiO_2	SO_4	Cl
1/5	4.86	4.38	10853	618	192	1238	217	2030	19822
2/101	4.47	13.19	10479	844	203	864	737	1300	19626
3/341	4.39	12.77	10404	975	271	717	754	851	19667
4/687	4.35	9.97	10695	797	295	659	785	936	19720
Q/706	6.0	-----	-----	633	659	812	473	1781	-----

	Fe	Mn	Zn	Cu	Pb	Ni	Cr	Co	Ba	Sr	Al	B	Au	Ti
1	1.54	56.8	2.3	----	----	0.50	----	0.02	0.08	2.8	0.31	8.5	0.09	0.01
2	1.60	605	2.1	----	----	0.35	----	0.02	0.08	3.4	0.22	22.4	1.30	0.01
3	2.10	614	2.2	----	----	0.30	----	0.02	0.14	4.3	0.26	24.0	1.40	0.01
4	5.70	582	2.9	----	----	0.48	----	0.02	0.18	4.5	0.29	24.0	1.30	0.01
Q	0.16	576	0.74	----	----	0.37	----	0.02	0.12	9.3	0.46	23.0	0.05	0.01

SM2 300°C

Sample/hr	pH	C iorg	Na	K	Ca	Mg	SiO_2	SO_4	Cl
1/2.0	2.71	7.98	10871	1044	109	562	2064	577	19904
2/79	2.34	7.31	10681	1201	184	272	2004	185	19760
3/261	2.73	8.00	10884	1281	176	255	1918	161	19998
4/573	3.02	7.66	10949	1380	181	208	1981	168	20051
5/1347	4.08	14.06	10874	1538	154	137	1246	146	19654
6/2811	4.17	12.15	10947	1317	135	114	1239	186	19376

	Fe	Mn	Zn	Cu	Pb	Ni	Cr	Co	Ba	Sr	Al	B	Au	Ti
1	5.9	520	9.6	2.7	0.53	0.25	0.04	0.24	0.22	1.3	0.12	17.5	1.20	0.01
2	6.7	756	16.2	11.5	----	0.43	0.04	0.09	0.38	2.0	0.12	22.6	1.70	0.01
3	4.2	777	16.4	43.8	5.75	0.40	0.05	0.09	0.49	2.3	0.17	23.0	1.70	0.01
4	1.3	807	19.0	54.5	3.50	0.50	0.07	0.06	0.42	2.8	0.17	23.1	1.80	0.01
5	0.2	700	17.6	57.7	0.52	0.45	0.01	0.03	0.41	2.9	0.21	23.8	1.66	0.01
6	0.2	657	17.4	60.3	0.41	0.54	0.01	0.02	0.44	2.4	0.18	24.3	1.60	0.01

Fluoride: 1 = 5.0, 2 = 6.1, 3 = 3.7, 4 = 3.0, 5 = 2.2, 6 = 1.1

#4 Pacific Smectite - 300°C

Sample/hr	pH	C iorg	Na	K	Ca	Mg	SiO_2	SO_4	Cl
1/3.5	2.50	5.09	10689	1023	59.9	746	1404	970	10198
2/73.5	2.90	9.27	10832	1297	139	341	2088	160	19260
3/315	2.95	11.55	10790	1347	109	293	2007	<150	19079
4/600	3.20	8.70	10993	1350	129	290	2068	<150	19079
5/1461	3.02	6.93	11011	1344	113	279	1959	<150	19352

	Fe	Mn	Zn	Cu	Pb	Ni	Cr	Co	Ba	Sr	Al	B	Au	Ti
1	-----	45.8	4.2	----	----	0.02	0.04	0.14	----	----	0.24	----	0.4	----
2	-----	132	15.2	----	----	0.05	0.10	0.17	----	----	0.19	----	99.6	----
3	0.45	118	18.2	----	----	0.15	0.09	0.12	----	----	0.14	----	96.1	----
4	0.07	114	19.3	----	----	0.02	----	0.11	----	----	0.16	----	84.0	----
5	0.15	104	19.8	----	----	0.02	0.12	0.10	----	----	----	----	85.5	----

Phosphorus: 1 = ---, 2 = 19.6, 3 = 11.6, 4 = 12.5, 5 =9.5 ppm

#5 Sediment B (San-200-5B) 200°C

Light brown clay composed of quartz, illite and Fe-chlorite, from MPG-1 study area.

Sample/hr	pH	C iorg	Na	K	Ca	Mg	SiO_2	SO_4	Cl
1/1.7	5.07	10.6	10341	558	461	1276	121	2469	19153
2/364	4.30	10.6	10609	734	168	863	462	1646	19303
3/675	4.39	10.6	10675	730	172	787	428	1626	19217
4/939	4.40	10.6	10944	705	305	578	433	1461	19347
5/1272	4.40	10.6	10763	706	224	725	445	1379	19398
6/1414	4.40	10.6	10781	729	221	683	460	1324	19148
Q/1437	6.85	----	-----	---	---	---	---	3056	19283

	Fe	Mn	Zn	Cu	Pb	Ni	Cr	Co	Ba	Sr	Al	B	Au	Ti
1	1.76	8.6	0.25	----	----	0.02	0.03	0.02	0.05	8.0	0.05	6.5	----	----
2	1.47	523	1.28	----	----	0.02	0.01	0.04	0.12	2.7	0.02	13.8	----	----
3	0.85	538	1.02	----	----	0.02	0.01	0.04	0.12	2.5	0.03	15.9	----	----
4	0.67	531	0.96	----	----	0.01	0.01	0.03	0.10	2.6	0.02	15.3	----	----
5	0.57	518	0.96	----	----	0.02	0.01	0.03	0.12	2.7	0.02	16.2	----	----
6	----	355	0.78	----	----	0.02	0.01	0.03	0.10	2.7	----	17.0	----	----
Q	----	----	0.16	----	----	0.04	0.01	0.03	0.08	11.7	----	17.1	----	----

Sediment B (San-300-5B) 300°C

Sample/hr	pH	C iorg	Na	K	Ca	Mg	SiO_2	SO_4	Cl
1/3.0	2.59	10.6	10676	747	64.1	926	1056	1605	19379
2/195	3.42	10.6	10759	1027	129	283	1099	463	19163
3/843	3.82	10.6	10885	917	154	184	982	231	19140
4/1242	3.87	10.6	11066	796	150	186	939	329	19253
Q/1247	5.78	----	11380	321	820	197	481	2037	19634

	Fe	Mn	Zn	Cu	Pb	Ni	Cr	Co	Ba	Sr	Al	B	Au	Ti
1	3.62	355	7.49	----	----	0.03	0.01	0.29	0.07	1.5	0.44	14.7	----	----
2	5.59	686	14.5	----	----	0.03	0.01	0.14	0.23	1.9	0.27	19.0	----	----
3	5.90	660	15.3	----	----	0.01	0.01	0.09	0.27	2.5	0.34	19.5	----	----
4	7.07	669	16.1	----	----	0.01	0.01	0.08	0.28	2.8	0.30	19.2	----	----
Q	1.13	586	2.6			0.08	0.03	0.05	0.21	11.7	0.25	16.4	----	----

---

#6 GPC3 200°C

Similar to SM2 but contains more metalliferous and amorphous material. Came from GPC3, 30°-19.9 min. N, 157°-49.4 min. W. (applies to both GPC3-13 and GPC3II experiments)

Sample/hr	pH	C iorg	Na	K	Ca	Mg	SiO_2	SO_4	Cl
1/1.0	5.07	5.44	11261	741	219	1040	417	1868	20102
2/123	4.00	8.29	11105	745	181	935	637	1449	19853
3/292	3.91	7.57	11071	870	190	921	625	1451	19897
4/674	4.74	7.46	11044	729	202	904	605	1402	19735
5/1389	4.05	8.10	11268	755	186	875	588	1411	19996
Q/1396	6.50	----	11580	571	550	1040	315	2692	20364

	Fe	Mn	Zn	Cu	Pb	Ni	Cr	Co	Ba	Sr	Al	B	Au	Ti
1	0.50	25.8	0.8	----	----	0.10	0.04	0.02	0.17	4.0	0.25	14.3	0.05	<.01
2	0.80	50.0	1.50	----	----	0.28	0.17	0.06	0.15	3.4	0.17	19.2	0.14	<.01
3	0.60	56.2	1.45	----	----	0.12	0.09	0.03	0.10	3.7	0.17	19.6	0.13	<.01
4	0.17	69.3	----	----	----	----	----	0.03	0.13	3.5	0.49	20.3	0.11	<.01
5	<.1	67.2	1.90	----	----	0.06	0.01	0.02	0.25	3.4	0.18	19.6	0.09	<.01
Q	<.1	62.9	<.1	----	----	0.01	----	0.01	0.20	9.4	0.42	19.9	0.06	<.01

GPC3 300°C

Sample/hr	pH	C iorg	Na	K	Ca	Mg	SiO_2	SO_4	Cl
1/3.0	3.35	12.17	10763	866	166	536	723	464	19967
2/93	2.38	12.31	10525	853	342	86.0	1121	54	19512
3/310	2.65	15.39	10512	1001	314	50.1	1262	54	19329
4/625	3.52	15.06	10584	961	322	49.1	1238	49	19352
5/1508	4.02	24.13	10289	880	356	50.8	1085	86	18785
6/3026	4.54	-----	10681	879	341	67.0	915	133	19423
Q/3045	5.90	4.92	-----	---	---	145	159	2202	19010

	Fe	Mn	Zn	Cu	Pb	Ni	Cr	Co	Ba	Sr	Al	B	Au	Ti
1	5.30	807	13.0	----	----	0.75	0.08	0.20	0.23	3.1	0.29	10.7	1.90	<.01
2	24.0	1113	13.6	----	----	0.50	0.16	0.12	0.85	6.8	0.34	13.2	2.70	0.01
3	2.70	1100	14.0	----	----	0.66	0.02	0.07	1.12	6.8	0.31	14.3	2.60	<.01
4	2.15	1117	14.0	----	----	0.55	----	0.06	1.00	6.9	0.36	14.2	----	<.01
5	1.00	1072	13.4	----	----	0.70	0.02	0.06	0.91	7.1	0.33	13.8	2.50	<.01
6	----	1125	----	----	----	----	----	----	----	---	----	----	----	----
Q	----	----	----	----	----	0.08	0.03	0.07	0.23	10.0	0.61	12.0	2.40	----

Fluoride 1 = 5.0, 2 = 3.9, 3 = 2.8, 4 = ---, 5 = 2.2, 6 = ----, Q = ----.

#7 GPC3 200° above the line - 300°C below

Sample/hr	pH	C iorg	Na	K	Ca	Mg	SiO_2	SO_4	Cl
1/3.0	4.80	4.54	9745	647	324	1128	355	1402	18444
2/74	5.10	6.67	9439	677	281	981	563	842	17894
3/267	4.60	6.77	9737	706	265	932	606	797	18262
4/602	4.30	7.44	10079	687	277	869	533	807	18613
5/648	2.94	6.86	10156	749	214	596	1165	295	18406
6/743	2.59	8.11	10280	1343	216	404	1501	230	18831
7/1017	2.50	6.10	9912	1408	212	365	1568	196	18330
Q/1056	6.30	----	10947	340	540	884	149	2553	18837

	Fe	Mn	Zn	Cu	Pb	Ni	Cr	Co	Ba	Sr	Al	B	Au	Ti
1	0.30	1.15	1.5	----	----	0.52	0.01	0.01	0.11	4.8	0.28	10.1	<.02	<.01
2	0.30	4.00	0.59	----	----	0.48	----	0.02	0.03	3.1	0.26	----	<.02	<.01
3	1.15	4.20	1.8	----	----	0.45	0.21	0.04	0.13	3.9	0.24	11.0	<.01	0.01
4	2.90	5.80	2.4	----	----	0.75	0.45	0.06	0.27	4.1	0.19	10.6	0.07	<.01
5	4.00	61.0	9.9	----	----	2.20	----	0.30	----	4.5	1.00	----	17.5	<.01
6	67	42.6	33	----	----	8	0.5	0.92	0.60	6.1	0.32	13.5	52.5	0.01
7	120	43.3	38	----	----	11	20	0.85	0.11	5.2	0.27	13.9	0.20	<.01
Q	0.16	1.45	0.61	----	----	0.60	0.16	0.10	<.01	10.0	0.48	12.5	0.02	<.01

Fluoride 1 = 0.7, 2 = 0.54, 3 = 0.44, 4 = 1.8, 5 = 1.7, 6 = 0.56, 7 = 2.3, Q = 7.5.

#8 CD 300°C

Organic-rich, slightly calcareous, olive-colored diatomaceous ooze composed of quartz, amorphous silica (diatoms), plagioclase and minor smectite and barite. From core BAV-79-E-10. 10 - 40 cm, 27°-52.3 min. N, 111°-39.7 min. W. - 644 m
water depth.

Sample/hr	pH	C iorg	Na	K	Ca	Mg	SiO_2	SO_4	Cl
1/1.0	3.25	9.87	11446	591	61	575	1755	1324	18983
2/74.5	4.00	16.96	11782	640	66	257	1702	622	18927
3/242	4.03	33.10	11968	662	89	206	1590	472	19329
4/697	4.73	>50	11735	677	188	123	1616	188	19237
5/1416	4.90	41.75	11592	674	301	69	1573	74	19083
6/2876	4.95	29.00	11579	656	426	68	1654	53	19299

Organic Carbon: 1 = 94.7, 2 = 80.3, 3 = 81.3, 4 = 72.8, 5 = 54.2, 6 = 50.2 - sample 6 also contained 1.63 millimolal methane.

	Fe	Mn	Zn	Cu	Pb	Ni	Cr	Co	Ba	Sr	Al	B	Au	Ti
1	39.3	5.7	4.5	<1	----	----	----	----	0.10	1.3	0.14	14.2	<.1	----
2	83.0	7.9	2.6	----	----	----	----	----	0.20	0.9	0.10	18.0	<.05	----
3	58.1	9.1	----	<1	----	----	----	----	0.23	1.7	0.11	18.9	0.03	----
4	13.5	9.3	<.5	<1	----	----	----	----	0.62	4.0	0.15	20.4	0.05	----
5	8.0	8.4	<.5	----	----	----	----	----	1.06	6.4	0.19	20.6	----	----
6	10.1	9.8	----	----	----	----	----	----	1.78	8.9	0.19	21.9	----	----

TABLE 2

Characteristics of Sediments Studied

Pre-test sediment analyses (weight %)

	Sed B	SM2	V36	CD	Pac. Sm	GPC3-13	GPC 3II
SiO_2	53.82	51.77	58.31	64.39	51.76	41.00	49.58
Al_2O_3	17.91	13.37	14.79	8.01	13.34	11.70	13.16
Fe_2O_3*	7.66	9.09	6.52	2.70	8.67	14.97	11.63
MgO	3.37	3.49	2.79	1.81	3.30	3.42	3.50
CaO	0.75	1.29	2.17	1.68	1.36	4.23	1.51
Na_2O	1.09	0.79	1.79	0.72	0.74	0.93	0.86
K_2O	3.92	3.71	2.63	1.48	3.82	2.45	4.42
TiO_2	0.84	0.59	0.70	0.33	0.63	0.56	0.56
P_2O_5	0.11	0.49	0.10	0.20	0.51	2.34	0.68
MnO	0.59	1.30	0.21	0.02	1.39	4.25	1.88
C- iorg.	0.0002	0.007	<.0001	----	0.012	0.050	0.020
C- org.	0.055	0.064	0.43	3.99	0.038	0.038	0.051
H_2O -	0.76	0.94	0.82	1.08	1.59	1.02	2.02
H_2O +	7.77	12.15	6.87	16.96	10.64	12.91	9.60

* Total iron expressed as Fe_2O_3

Trace Elements In Parts Per Million

Ba	1032	381	681	519	407	655	419
Co	77	45	27	5	53	240	67
Cr	110	43	79	49	57	36	38
Cu	196	276	112	29	283	540	310
Ni	107	152	47	35	178	365	202
Pb	35	42	28	34	45	68	50
Sr	162	203	159	145	217	347	208
Zn	133	165	101	74	173	224	185

2.0 EXPERIMENTS IN A TEMPERATURE GRADIENT

The second topic investigated concerned the influence of thermally driven transport mechanisms on the chemical reactions studied previously under isothermal conditions. Basically these can be divided into two categories, Soret transport and convectively driven fluid flow. In the first process the extent of transport can be characterized by the Soret coefficient, s, defined by the following equation:

$$F = -D(dC/dz + sCdT/dz) +R, \qquad \text{(Eq. 2.1)}$$

where F is the flux of a component through a reference interface, D the Fickian diffusion coefficient of that component, dC/dz is the concentration gradient, dT/dz the temperature gradient, and R is a source-sink term for the production or consumption of that component. In instances where no reaction occurs (R = 0) and the system has reached a steady state (F = 0) the equation may be integrated to yield:

$$\ln(C/C') = -s(T-T'), \qquad \text{(Eq. 2.2)}$$

where the C and C' are the steady state concentrations at two localities having temperatures T and T' respectively. It is important to note that at steady state the geometric factors have dropped out of the equation. This reflects the fact that an equilibrium condition has been reached. Consequently, although one-dimensional experiments in long autoclaves proved ideal for determining numerical values of s, the equation can be applied with equal validity to any system where chemical separation occurs in response to an imposed temperature gradient, and where the concentrations have reached a steady state. A more serious problem arises from the the ionic nature of electrolyte solutions. Although individual ions may respond differently to a temperature gradient the necessity of maintaining electrical neutrality results in a cross coupling between the motion of all ionic species in solution. As a working approximation in this study chloride was regarded as the only important anion and the overall process was treated as the summed transport of various chloride salts.

The other important thermal transport mechanism studied was fluid convection. Unlike Soret transport, geometric factors remain important for as long as the process operates. Experiments must then be constructed so that in some sense they may be scaled to match the geometry of the actual system of concern (e.g a buried waste canister). A second important difference is that, unlike the Soret effect, convection has the potential for delivering large amounts of material to the hottest part of a system. Thus, one important unknown regarding such systems was whether magnesium uptake would proceed so vigorously that very acidic solutions result, or alternatively whether free communication with a large mass of unreacted seawater and sediment would so buffer such systems that the pH never falls much below neutrality.

2.1 Soret Transport

To obtain values for Soret coefficients a titanium lined autoclave was used and a temperature gradient imposed that ranged from 300 to 100°C over

the 30 cm length of the apparatus (4, 13, 21). Pressure was maintained at 600 bars except during sampling. As samples were obtained from both hot and cool ends of the autoclave, it was possible to evaluate when a steady state separation had been achieved. Soret coefficients for various components could then be evaluated using the integrated form of the transport equation. The other problem to be overcome was that of chemical reactions that might add or remove components from solution. For the major cations in seawater this was accomplished by preparing an artificial sulfate-free seawater substitute and filling the autoclave with inert 3-micron alumina in place of sediment. Although noticable enrichments in chloride, potassium, magnesium, sodium, and calcium were found in the cool end after four days, 25 days were required to reach steady state (Table 3, entry #1). At that time the thermally induced separation had produced a high-temperature fluid with roughly half the ionic strength of cool fluid. The actual Soret coefficients obtained from this control experiment are summarized below (Table 4, column 1). In general, these values were somewhat higher than those found at lower temperatures by Caldwell and Eide (22). This is, however, consistent since the lower temperature data (Table 4, Column 2) also exhibits an increase with temperature that asymptotically approaches a value of about 0.004 per °C in the 100 to 300° range (23).

Similar experiments using actual sulfate containing seawater and reactive V36 sediments showed an interesting mix of Soret transport processes and rock-water interactions (Table 3, Entry #2). For example, potassium concentrations at both ends increased initially because the temperature rise caused a shift in the ion exchange equilibria. At the hot end poorly crystallized illitic clays also dissolved quickly, contributing additional potassium and silica to solution. Once these sources were exhausted, Soret transport took over. By the end of the experiment potassium had been redistributed so effectively that the Soret coefficient was almost the same as when an inert matrix was used (Table 4, Column 3). Reactions involving magnesium were slower and continued until the end of the run. As a consequence magnesium appeared to have an anomalously large Soret coefficient. The same situation existed with calcium, probably because of the continued precipitation of anhydrite at the hot end of the autoclave. It also appears that silica moved toward the cool end, though whether this was a manifestation of the Soret effect or just the higher concentrations achieved at the hot end of the autoclave remains unknown. In any case, this might have delayed the onset of smectite precipitation, thus accounting for the slow drop in pH as compared to the rates noted during isothermal studies. A second factor to be considered, however, is the proximity to the near-field zone of unheated sediments and seawater. These materials have a significant buffer capacity which, until titrated, preclude development of an acidic condition.

One final aspect of gradient-induced transport concerns several experiments where a borosilicate glass waste-form simulant (PNL-76-68) was placed in the hot end of the autoclave along with the normal load of seawater saturated sediment (Table 5). Although directly relevant to a prematurely failed canister, this data is also of interest because it expands somewhat the number of elements studied in a thermal gradient. As expected, the glass devitrified completely during the experiment to a mixture of clay (rich in smectite), ruthenium dioxide, acmite, paragonite,

anhydrite and iron oxide, while the oxidizing effects of the of the glass were manifested as a dark reddish-brown coloration for about 3.5 inches along the core (total length 10 inches). A similar core from the GPC experiment (Table 5, Entry 2) was also divided into seven sections and analyzed. Surprisingly, even relatively immobile elements such as Cr and the rare earths moved, reaching their peak concentrations in the second section of core away from the glass (255°C). The surprising mobility of these elements suggests that the rapidly altering glass temporarily created conditions that were optimal for the formation of polynuclear ionic species. Once formed, such species are relatively stable (24, 25) and apparently migrated for some distance before breaking down. Although Zn, Sr, Zr, Ba, and U do not exhibit concentration maxima away from the glass, they also showed evidence of mobility. In fact, significantly elevated concentrations were found in sediments as far away as the fifth segment out from the glass (220 - 195°C). Finally, as would be expected from the behavior of other alkali metals, Cs and Rb actually increase toward the cool end of the autoclave. Fluid samples from the cool end also contained anomalous concentrations of B, Mo, and Cs derived from the glass. Although both concentration and temperature gradients undoubtedly played a role in this transport, the important point is the degree to which individual elements were separated one from the other. Given several decades, instead of months, such processes might similarly affect the minor components in relatively unreactive sediments. As these zones would then persist indefinitely, the problem of defining the term "near field" would also persist long after the sediments have cooled. This, in turn, would require a more detailed description of the cooled sediment than merely documenting where major mineralogic changes had occurred.

TABLE 3

A Comparison of Temperature Gradient Induced Transport in Reactive and Nonreactive Systems.

#1 Sulfate-Free "Seawater" and Inert Matrix of Alumina

Soret Experiment - 100°C - Cool End

Sample/hr	pH	C iorg	Na	K	Ca	Mg	SiO_2	SO_4	Cl
initial	7.85	2.25	9214	359	395	1661	----	----	19994
1/1	7.18	----	9467	390	396	1644	----	----	20373
2/28.5	4.31	----	9577	393	393	1673	----	----	19654
3/99.0	5.80	----	9853	405	417	1698	----	----	21221
4/337	6.52	----	10323	449	441	1790	----	----	22321
5/503	6.40	----	10641	467	464	1837	----	----	22955
6/673	6.57	2.8	10838	475	481	1888	----	----	23423

Soret Experiment - 300°C - Hot End

Sample/hr	pH	C iorg	Na	K	Ca	Mg	SiO_2	SO_4	Cl
initial	7.85	2.25	9214	359	395	1661	----	----	19994
1/1	6.86	----	9140	388	371	1586	----	----	19654
2/28.5	6.90	----	9429	414	401	1501	----	----	19932
3/99.0	5.67	----	8788	365	378	1425	----	----	18684
5/503	5.31	----	5629	186	172	700	----	----	11186
6/673	5.58	3.3	4918	203	184	746	----	----	10244

#2 Transport in a reactive system containing V36 Sediment and Actual Seawater

Sediment Gradient Experiment - Cool End - 100°C

Sample/hr	pH	C iorg	Na	K	Ca	Mg	SiO_2	SO_4	Cl
SW.0	7.9	2.33	10763	399	412	1297	<.2	2734	19375
1/21.5	6.02	3.45	11050	628	427	1237	250	2773	19900
2/101.5	5.62	3.93	11866	740	423	1244	422	2923	21144
3/284.5	5.39	4.07	13136	874	393	1204	593	2891	23179
4/504	5.31	4.33	13589	975	396	1184	644	2676	24088
5/768	5.19	5.27	13801	1015	356	1170	684	2559	24443
6/1296	4.95	5.41	14045	1047	357	1120	714	2450	24786
Q/1302	----	----	13397	911	346	1111	566	2599	23490

	Fe	Mn	Zn	Ba	Sr	Al	B	U	Cs	Mo
1	<1	19	<3	<2	8.5	<.5	6.5	<5	<.1	<1
2	2	35	3	<2	8.5	<.5	7.1	<5	0.2	<1
3	<1	53	<3	<2	7.3	<.5	8.5	<5	0.4	<1
4	<1	67	<3	<2	7.0	0.5	8.9	<5	0.5	<1
5	<1	79	---	---	6.8	---	9.3	<6	0.2	<1
6	<1	95	---	---	---	---	---	---	---	---
Q	11	79	---	---	---	---	---	---	---	---

Sediment Gradient Experiment - Hot End - 300°C

Sample/hr	pH	C iorg	Na	K	Ca	Mg	SiO_2	SO_4	Cl
1/21.5	7.88	2.59	11153	581	302	1173	52	2442	19764
2/101.5	5.00	13.12	11473	1102	222	257	679	442	19219
3/284.5	4.11	12.70	9621	841	155	142	875	239	15673
4/504	3.51	10.12	8158	657	114	131	820	220	13373
5/768	3.36	10.17	6626	464	97	131	1178	213	10942
6/1296	3.26	8.29	7062	491	96	173	961	217	11758

	Fe	Mn	Zn	Ba	Sr	Al	B	U	Cs	Mo
1	<1	6	<3	<2	6.0	<.5	5.8	<5	<.1	<1
2	176	1613	14	5	3.6	<.5	17.5	---	<.1	<1
3	183	128	12	<2	2.4	<.5	15.2	<5	<.1	<1
4	120	99	5	2	0.6	<.5	11.1	<5	<.1	<1
5	90	84	---	---	<2	---	9.4	<5	<.1	<1
6	89	79	---	---	---	---	---	---	---	---

TABLE 4

Soret Coefficients x $10^3(C^{-1})$

	100° - 300°C Control	35°C Cl Salt Av.	100° - 300°C Sediment	5 - 150°C ISIMU
Chloride	4.1	---	4.0	4.3
Sodium	4.0	2.3	3.7	3.1
Magnesium	4.6	2.8	10.9	15.1
Potassium	4.3	---	3.9	0.9
Calcium	4.8	3.6	6.5	9.7

Column 2: Caldwell, D. R. and S. A. Eide, (22)
Columns 1 and 3: Thornton, E. C. and W. E. Seyfried, (21)
Column 4: Seyfried, W. E., E. C. Thornton, and F. L. Sayles, (23)

TABLE 5

Transport in Reactive Systems to which a Glass Waste Form Simulant Is Added

#1 Gradient Experiment With PNL-76-68 Glass and GPC-3 Sediment - Cool (100°C) end data only.

Sample/hr	pH	C iorg	Na	K	Ca	Mg	SiO_2	SO_4	Cl
1/29	5.0	-----	12094	545	459	1335	69	2875	21698
2/192	5.4	3.03	13320	822	512	1407	111	3205	23897
3/405	5.4	5.24	14793	875	521	1336	158	3283	25965
4/740	5.5	3.79	15728	903	472	1278	208	3494	27005
5/1032	5.7	5.29	15424	1074	453	1173	280	3528	26280
6/1370	6.0	5.73	15488	993	420	1097	310	3415	26120
7/1757	5.8	5.17	14609	1070	388	994	367	3291	24578
8/2068	5.5	4.86	14910	992	369	940	438	3091	24992
9/2475	5.0	5.04	14670	1038	355	887	493	2934	24610
10/2925	5.3	5.08	14774	1062	358	809	461	2889	24593
Q/2980	5.5	----	14870	950	357	874	415	2857	24849

	Fe	Mn	Zn	Ba	Sr	Al	B	U	Cs	Mo
1	<10	3.9	<1	---	8.9	---	5.6	<5	---	---
2	<10	5.5	<1	---	10.7	---	11.9	<5	0.8	<1
3	<10	3.0	---	---	12.4	---	112	<5	6.6	<1
4	<10	3.8	---	---	11.6	---	279	<5	30	<1
5	<10	3.0	---	---	11.5	---	389	<5	68	<1
6	<10	3.2	<1	---	8.9	---	432	<5	99	<1
7	<10	3.6	<1	---	9.2	---	480	<5	100	1
8	2.7	3.2	---	---	9.6	---	451	<5	77	16
9	3.9	4.2	---	---	9.5	---	440	<5	77	16
10	2.3	6.6.	---	---	8.8	---	444	<5	81	16
Q	2.6	5.6	---	---	---	---	378	>5	66	15

Corrected analytic data for seven splits of GPC3-G core normalized to 13.2 percent alumina, and the reacted glass to 2.9 % titanium dioxide. Temperatures given are approximately those experienced by that section of core during the experiment.

	GPC3II	G-1	G-2	G-3	G-4	G-5	G-6	G-7	76-68	Glass
T(°C)		135	160	195	220	230	255	275	300	
SiO_2	47.62	49.11	47.54	49.73	49.92	48.25	46.78	53.58	21.13	37.95
Al_2O_3	13.20	13.2	13.2	13.2	13.2	13.2	13.2	13.2	1.45	0.32
Fe_2O_3	11.41	11.24	11.09	11.33	11.19	11.24	11.25	11.46	11.55	10.94
MgO	3.41	3.82	3.43	3.49	3.45	3.81	4.30	6.79	1.62	0.06
CaO	1.48	1.47	1.40	1.32	1.30	1.87	1.98	1.68	1.38	1.98
Na_2O	3.18	12.49	9.39	7.10	5.53	5.64	5.38	5.68	1.38	12.79
K_2O	3.38	3.86	3.68	3.59	3.48	3.28	2.63	2.39	1.01	0.06
MnO	1.83	1.83	1.77	1.78	1.63	1.63	1.63	1.88	0.12	0.05
TiO_2	0.51	0.53	0.51	0.53	0.53	0.55	0.55	0.57	2.90	2.90
B_2O_3	0.06	0.67	0.59	0.57	0.50	0.56	0.54	0.41	0.15	9.15
H_2O*		22.34	18.68	15.32	13.44	14.64	13.95	10.55	6.34	1.65

total iron + expressed as Fe_2O_3
* $H_2O = H_2O + H_2O$

Trace Element (ppm) and FeO and Na_2O (%) determinations of sediment samples from thermal gradient experiment GPC3-G by neutron activation analysis.

Na_2O	2.58	9.85	8.45	6.48	5.32	5.29	5.33	5.32
Cr	2.93	28.2	30.6	34.1	41.5	62.5	114.8	63.1
FeO	9.36	8.22	8.56	8.95	9.40	9.43	9.58	9.37
Ni	250	200	200	160	186	220	230	280
Br	43	---	158	115	93	92	85	57
Rb	88	145	138	138	137	135	129	130
Sr	202	270	280	240	216	320	460	650
Zr	246	210	260	300	670	850	1220	1690
Cs	4.6	970	700	520	410	339	304	367
Ba	320	302	340	360	280	270	470	970
La	94.6	84.3	87.5	93.7	110.9	121.9	153.3	151.1
Ce	117.5	M02	105.8	114.7	147.5	186.1	263.8	250.0
Nd	106	97	97	105	143	184	295	248
Sm	28	24	26	26	29	38	57	41
Eu	5.9	5.4	5.6	5.8	7.0	9.0	13	11
U	2.1	2.1	3.8	42	168	235	337	580

#2 Gradient Experiment with PNL-76-68 Glass And V36 Sediment - Cool (100°C) End Data

Sample/hr	pH	C iorg	Na	K	Ca	Mg	SiO_2	SO_4	Cl
1/17.5	5.60	3.79	11138	614	428	1227	319	2640	20115
2/117	5.15	5.33	12142	751	270	1142	657	2308	21538
3/282	5.05	5.80	12871	805	259	1100	718	2188	22663
4/500	4.81	5.64	13285	877	255	1001	806	2167	23086
5/741	4.62	5.88	13497	900	243	926	847	2009	23303
6/1196	4.58	5.07	13904	953	270	814	800	1991	23699
7/1649	4.57	4.71	13996	988	273	738	827	1806	23791
Q/2103	----	----	14160	998	257	654	801	1608	23919

	Fe	Mn	Zn	Ba	Sr	Al	B	U	Cs	Mo
1	2	1	<3	<2	10	<.5	1019	<5	241	371
2	<1	1	<3	<2	4.8	0.5	----	<5	171	<30
3	<1	1	<3	<2	7.9	<.5	758	<5	75	18
4	<1	<1	<3	<2	4.6	<.5	370	<5	43	8
5	3	7	4	2	4.7	<.5	266	<5	32	7
6	2	4	6	3	7.8	<.5	214	<5	35	1
7	3	<1	13	5	7.4	<.5	186	<5	29	<1

Gradient Experiment with PNL-76-68 Glass And V36 Sediment - Hot (300°C) End Data

Sample/hr	pH	C iorg	Na	K	Ca	Mg	SiO_2	SO_4	Cl
1/ 17.5	6.94	10.78	12057	640	23	55	299	1331	18066
2/ 117	6.47	25.4	9556	653	6	<5	1081	656	14271
3/ 282	5.81	17.4	8203	608	17	<5	1136	375	12792
4/ 500	5.28	11.9	7108	544	24	<5	1216	141	11368
5/ 741	4.77	10.54	7383	526	69	<5	1252	111	11916
6/1196	4.93	6.78	7287	506	106	<5	1144	85	11838
7 1649	5.05	6.91	7173	479	128	<5	1132	50	11701

	Fe	Mn	Zn	Ba	Sr	Al	B	U	Cs	Mo
1	1	19	<3	<2	7.9	<.5	6.4	<5	0.6	<1
2	4	38	3	<2	5.6	<.5	35	<5	1	<1
3	8	47	3	<2	6.3	<.5	158	<5	15	<1
4	12	49	3	<2	6.1	<.5	225	<5	23	<1
5	15	48	<3	<2	6.0	<.5	223	<5	35	1
6	21	45	<3	<2	6.7	<.5	217	<5	46	3
7	22	45	<5	<2	7.8	<.5	202	<5	58	5
Q	25	46	---	---	---	---	---	---	---	---

2.2. Combined Convection and Soret Transport

The In Situ Heat Transfer Simmulation Experiment (ISIMU) provided, among other things, a chance to study geochemical and mass transport processes on a larger scale and in a more complex geometric setting then was previously possible (4, 13, 23). For this study a cylindrical heater (2 cm diameter) was placed vertically into a 1 cubic meter tub of illitic quartz-rich sediment. This, in turn, was covered by a reservoir containing about 2 cubic meters of artificial seawater (sea-salt solution). The heated section of the probe was about 12 cm long and the top of the heated section was roughly 20 cm below the sediment-seawater interface. A large autoclave was employed to maintain a pressure of about 50 MPa. Hence, boiling was prevented even though the heater surface reached 270°C. After 30 days pore fluid samples were taken at five locations along the temperature gradient. The experiment was then terminated and the sediment examined for mineralogic and textural changes.

The most obvious change was a baked zone which developed within about 3 cm of the heater (23). Baked sediments were more consolidated than unheated material, had significantly higher shear strengths, and had higher water contents showing evidence of enhanced permeability. Presumably, this water resided in numerous microcracks. The mineralogy and bulk chemistry of the baked sediment were also altered (Table 6, Entries 1 and 2). It contained less quartz, illite, and kaolinite than the starting material, and was a bleached gray color due to the reduction of ferric iron by organic material. K-feldspar and Mg-rich chlorite were more abundant than in the initial sediment. Of greater importance, though, was the presence of a new mineral, analcime. In the sediments altered at 185, 220, and 270°C the analcime content was about 10%, 20%, and more than 30% respectively. Even a crude mass balance calculation demonstrates that the pore water in this region could not have supplied enough sodium to account for this change. Instead, it is likely that convection caused fresh seawater to circulate downward from the overlying reservoir. Analcime precipitation also requires a relatively high Na/H ratio and, like chlorite, silica concentrations at, or below, quartz saturation. Active convection could also account for both these environmental constraints. Fluid in the cool reservoir apparently contained more than enough alkalinity to titrate the hydrogen ions produced during chlorite formation. At the same time the fact that quartz dissolution is a relatively slow process meant that while active circulation continued the solution would also retain the low silica concentrations conducive to chlorite and analcime formation (26,27). Finally, in the upper part of the convective cycle, dissolved silica would be removed to the overlying seawater reservoir, thus accounting for the bulk silica depletion apparent in post-test analysis of baked sediment.

Beyond the margins of the baked zone (T< about 185°C) additional mineralogic reactions occurred, though the effect on the appearance of the sediment was less dramatic. Significant elemental trends in this region included a maximum in the silica content at the boundary between baked and unbaked sediment, and a peak in MgO at about the 130°C isotherm. These correspond to sediments that gained quartz and chlorite respectively. Pore fluid samples were also obtained from this region (Table 6, Entry 3), and provide additional insight into the geochemical processes occurring there. Because of geometric constraints the maximum temperature of a pore fluid sample was 150°C, and the minimum temperature was 5°C. The distribution of

magnesium concentrations found at various temperatures suggests, as usual, a Soret coefficient that is anomalously high (Table 4, Column 4), thus confirming the ongoing production of new chlorite. For sodium and potassium the opposite is true, indicating that a source for these elements existed in the high temperature end of the experiment. The obvious guess is that they may be coming from the freely circulating reservoir of seawater in the adjacent baked zone. It is perplexing, however, that chloride apparently exhibits no evidence of an anomalous source at the higher temperature. An explanation consistent with all the facts is that excess sodium and potassium came from early reactions near the baked/unbaked zone boundary. Possibilities include ion exchange with the clays or ions liberation during feldspar dissolution.

TABLE 6

Results from ISIMU Test

Entry #1 - Mineralogy Of Sediments From Various Temperature Zones

Mineral	Temperature (°C)					
	30	85	130	185	220	270
				<- Baked Zone ->		
Quartz	S	S	S	M	S	t
Illite	M	M	M	M	S	S
Fe-chlorite	S	S	M	S	S	S
Plagioclase	S	S	S	S	S	S
K-feldspar	m	m	m	m	m	S
Kaolinite	S	S	S	m	m	m
Analcime	-	-	-	m	S	M
Anhydrite	-	-	-	-	-	t

M = Major Component, 30% or more S = Subordinate, roughly 15%
m = Minor Component, 5% - 15% t = Trace, only a main peak is seen
- = None Detectable by X-ray Diffraction

The sediment used in this test was a marine clay from the North Pacific Basin composed of illite, quartz, feldspar and Fe-chlorite with minor amounts of smectite, cristobalite, barite, hematite and forsterite.

Entry #2 - Solid sediment analyses from the ISIMU experiment

	GC - 1	GC - 2	GC - 3	GC - 4	GC - 5	GC - 6
SiO_2	56.88	56.78	55.30	56.60	54.35	51.60
Al_2O_3	18.12	18.05	17.56	17.38	18.50	19.07
Fe_2O_3	6.68	6.61	6.47	5.72	6.31	6.02
FeO	1.15	1.19	1.09	1.55	1.37	2.04
MgO	3.53	3.52	5.64	4.24	4.49	4.56
CaO	0.87	0.82	1.04	1.10	1.28	1.65
Na_2O	1.21	1.22	1.14	2.03	2.40	5.34
K_2O	3.69	3.64	3.53	4.00	4.33	3.55
TiO_2	0.86	0.86	0.84	0.84	0.88	0.88
P_2O_5	0.13	0.13	0.12	0.12	0.12	0.11
MnO	0.41	0.41	0.42	0.43	0.42	0.50
CO_2	0.22	0.22	0.23	0.42	0.40	0.08
H_2O	7.63	7.79	8.70	6.07	7.19	6.14

Entry #3 - ISIMU Fluid Analyses

T(C)	pH	Alk.	Na	K	Ca	Mg	SiO_2	SO_4	Cl	Mn	Fe
25*	8.00	3.3	0700	410	333	1450	< 1	2750	19860	<1	<1
5	7.39	2.06	10660	411	323	1446	5.0	2146	19956	<1	<1
15	6.55	2.97	9406	367	277	1258	9.1	1941	17462	<1	<1
27	6.70	3.29	9314	483	347	1050	33.8	2296	16708	1.4	<3
47	7.10	3.76	8405	480	309	879	32.7	2006	14899	1.4	<3
70	8.90	3.05	9200	403	291	1144	20.6	1908	16890	3.4	<3
125	8.85	3.82	7177	419	134	279	94.2	1096	11566	22.4	<3
150	7.88	5.10	6340	346	74.5	149	105	795	9883	4.6	<3

*Pre-Test Fluid Composition

3.0 RADIATION EFFECTS IN THE NEAR FIELD

The intense gamma radiation adjacent to a waste canister raises questions which obviously cannot be addressed by resorting to conventional geochemical analogues, and which also go beyond the scope of the relatively scant literature on the irradiation of natural materials (28, 29, 30, 31). First, and perhaps foremost, was whether the basic mechanisms governing sediment - seawater interactions would be altered by an intense dose of ionizing radiation. While ample data attest to the stability of clays during dry gamma irradiation treatments (30, 31), it was less clear what would happen to clays suspended in a reactive fluid at high temperatures. A second question was whether unusual radiolysis products would come to dominate the pore fluid chemistry. Again, though data exist for the simple irradiation of brine (28, 32), it was not clear how these could be applied to clay - seawater suspensions at high temperatures. Under the heading of radiolysis products two general areas were of concern. On one hand, high concentrations of oxidizing agents (NO_3^-, ClO_3^-, H_2O_2) might enhance canister corrosion rates. Alternatively, reduced hydrogen gas might build up to the extent that a titanium - based canister material could be affected by hydrogen embrittlement. The second topic of concern is synergistic effects on overall system performance. For example, if radiolytic gases were produced rapidly enough bubbles might nucleate. This, then, could interfere with heat transfer from a canister causing anomalously high temperatures or a tendency for the canister (plus near field sediments) to "float" toward the sediment-seawater interface.

3.1 Isothermal Seawater-Sediment-Radiation Interaction Studies

To accomodate the large number of sediment types of interest small (3.7 ml internal volume) closed Ti Code 12 autoclaves were designed for use in the Sandia LICA (low intensity cobalt array) facility. These autoclaves were equipped with a rupture disk which, at the conclusion of an experiment, could be punctured in a specially designed vacuum chamber. Thus, samples of radiolytic gases could be taken directly into a gas chromatograph for analysis. Because these were constant volume autoclaves, a head space was left to accommodate the expansion caused by heating. This void space also allowed radiolytic gases to escape from solution into the vapor phase. The sediment-seawater mixtures treated in this manner are summarized below.

TABLE 7

Conditions Of Irradiation For Various Sediment Types

Smectite + Illite	Air Dried	127°C	$3x10^{10}$Rads	
Illite Rich	"	"	"	
Calcareous Ooze	"	"	"	
Smectite + Illite	P. Sat.	150°C	$2x10^{8}$ Rads	" Pac. Sm "
Illite + Smectite + Clinoptilolite	P. Sat.	127°C	$1x10^{10}$Rads	" Pac. Sm "
Atlantic Calcareous Ooze, calcite + quartz, trace organic material, illite and kaolinite	P. Sat.	200°C	$1x10^{8}$Rads	" GME "
Atlantic Silty Clay illite + kaolinite + chlorite + quartz, trace dolomite, organic matter	P. Sat.	200°C	$.6x10^{8}$Rads	"SNAP "
Pacific Red Clay illite + kaolinite + quartz + chlorite	P. Sat.	200°C	$.6x10^{8}$Rads	"VEMA "
Pacific Red Clay Illite + kaolinite + quartz + chlorite	50 MPa	300° - 40°C.	$5x10^{8}$ Rads	

P. Sat indicates that the pressure on the system was essentially that of boiling seawater with a slight addition from the radiolytic gases.

3.1.1 Mineralogy and Solution Chemistry

One may easily generalize regarding radiation effects on sample mineralogy: None, or at least not any detectable by routine x-ray diffraction analyses. All mineralogic changes noted could be ascribed to the hydrothermal conditions alone. These included: 1) illite and smectite recrystallization, 2) anhydrite precipitation, and 3) removal of calcite from GME sediment and dolomite from the SNAP sediment. During the radiation treatments a sample of bentonite was also run to serve as a control (30). This clay is better crystallized than marine smectite, so it was thought that small changes would be more noticeable in such samples. However, like the marine clays, no changes were observed that could be ascribed to radiation.

For SNAP, VEMA and GME experiments analyses were also obtained of the quenched post-irradiation fluids. The trends noted in these experiments include:

1) A large increase in calcium and bicarbonate coupled with a decrease in magnesium in both SNAP and GME sediments. Acid generated by magnesium smectite formation or the breakdown of organic compounds at elevated temperatures apparently reacted with the carbonate minerals in the sediment.

2) Modest increases in sodium and chloride, probably arising from a combination of ion exchange reactions with clays and evaporation when the samples were opened under vacuum for gas analyses.

3) A fairly large increase in potassium, probably arising from temperature-induced ion exchange reactions with the clay.

4) Elevated iron and aluminum concentrations, possibly reflecting organic complexes (10) or, alternatively, the difficulty in filtering very finely divided colloidal material from samples.

5) An increase in silica reflecting the higher solubility of silica polymorphs at higher temperatures, and possibly it's liberation during seawater-sediment chemical reactions.

In general, the solution chemistry data adds additional weight to the conclusion that gamma radiation does little to effect the normal course of hydrothermal clay-water interactions. Similar changes in solution chemistry were found in both irradiated and unirradiated experiments, which in turn also closely resemble those already discussed in Section 1 of this report. To eliminate the dominant overprint of hydrothermal effects a second set of control experiments was carried out at room temperature. Except for calcium in the GME experiments, the room temperature irradiation seems to have left solution compositions unchanged. This slight increase in calcium is probably related to organic acid production in the radiation field. The probability that a similar increase was not observed in the case of the SNAP sediment, reflects the predominance of calcite over dolomite in this sample. It seems, then, that any concerns regarding the possibility of

radiation enhanced seawater-clay reactivity in hydrothermal environments are unfounded.

TABLE 8

POST-TEST SOLUTION COMPOSITIONS (PPM) AFTER 14 DAYS OF TREATMENT

T °C 10	Dose Rads	pH	Cl	HCO_3	SI	Fe	Ca	Mg	Al	K	Na
		<----------					ppm				---------->
					GME SAMPLES						
200	1.08	7.2	----	370	97	1.8	2,240	206	2.9	580	12,400
200	0.60	7.2	----	310	97	2.3	2,240	220	2.9	570	12,700
200	0	6.1	23,600	---	105	1.0	3,110	220	3.5	640	12,100
25	1.45	6.8	21,000	---	23	1.2	830	1,290	1.3	530	11,100
25	0.60	6.7	18.600	---	12	0.7	750	1,260	1.5	560	10,600
					SNAP SAMPLES						
200	0.64	7.3	----	350	79	0.8	1,980	340	4.4	590	12,700
200	0.60	7.4	----	320	56	1.2	1,620	815	2.1	560	13,400
200	0	5.9	----	---	60	10	2,030	380	2.7	575	11,200
25	1.09	6.6	21,300	---	7.5	1.1	430	1290	1.1	463	11,200
25	1.03	7.1	22,100	---	13	1.1	440	1310	1.0	476	11,000
					VEMA SAMPLES						
200	1.43	6.3	----	100	110	0.9	560	1100	1.0	631	12,200

3.1.2 Radiolysis Effects

The next matter to be addressed is the extent to which radiolysis may influence the chemistry of such systems. One measure of the intensity of such process is the "G value", which measures the number of molecules formed for each 100 ev of gamma ray energy deposited in the sample. For molecular hydrogen the G value is typically between 0.45 and 0.50 for measurements made below 160°C, but at least for brines, it increases to approximately 0.8 between 170 and 180°C (28, 32, 33). From a programmatic standpoint, it is fortunate that this parameter is so well studied since it may be used as a yardstick to judge whether anomalous radiolysis processes are occurring. Further, since radiolytic oxygen from the dissociation of water is the primary feed for the production of other oxidizing agents, the amount of radiolytic hydrogen places limits on the extent of radiolytic oxidizing agent production. To obtain the G values presented below (Table 9), the amount of gas in the autoclave was determined following irradiation. This was then combined with dose estimates to evaluate the ratio between gas production and energy absorbed.

Several aspects of this data are of interest. First, with increasing dose the tendency to produce molecular hydrogen gas falls off both with and without sediment in the system. This can readily be ascribed to the buildup of radiolysis products in the head space over the fluid, which in turn increases the rate of recombination reactions. A coupled problem is what would happen were the head space entirely eliminated. This was evaluated by comparing two room temperature experiments, one with a completely full autoclave and another partly filled in the usual manner (Table 10). As expected (28), confining the radiolysis products to the liquid phase increased the rate of recombination reactions. Secondly, all the G values for hydrogen gas are significantly below the optimal value of 0.45. Hence, if anything, the presence of suspended clay increases the recombination rate of hydrogen and oxygen. Finally, there are some obvious trends in the types of gases produced from the various sediments tested. For highly oxidizing red clays the ratio of hydrogen to oxygen (plus the small amount of carbon dioxide) in the head space gases closely approximates 2. This would be expected if water were being quantitatively dissociated and the only sink for oxygen was the oxidation of the small amount of kerogen in the sample. This finding mitigates strongly against much production of aqueous oxidizing agents (H_2O_2, ClO^-_x, NO^-_x, etc.), since oxygen is not obviously missing from these head space gases. This was confirmed by adding a small amount of sodium iodine to the irradiated solutions. In the presence of aqueous oxidizing agents molecular iodine forms and a distinctive reddish-brown color develops. No such color change was observed, thus limiting the concentration of aqueous oxidizing agents (or at least those long lived enough to survive until the autoclaves were opened) to below about 10^{-4}molar. When more organic-rich sediments were irradiated, hydrogen and carbon dioxide were the principal gases formed while molecular oxygen was generally absent. With such sediments, the missing oxygen may either go into making carbon dioxide or into less fully oxidized organic compounds such as alcohols or organic acids. In evaluating these two possibilities it was found that the amount of calcium in solution after the treatment agreed reasonably well with the amount of carbon dioxide found in the head space, which in turn, somewhat exceeded the amount of missing oxygen. Thus, most

of this carbon dioxide probably originated from the acidic dissolution of carbonate minerals. One might then speculate that the missing oxygen went into the production of water soluble organic compounds. If some of these were organic acids, they might have then contributed to carbonate dissolution along with the acid produced during production of Mg-rich sheet silicates.

To summarize, radiation seems to have little effect on the overall course of rock-water interactions. Where the sediment maintained highly oxidizing conditions, the only significant radiation effect was the radiolysis of water to produce a mixture of hydrogen and oxygen gas. High concentrations of dissolved oxidizing agents were not found, nor was the production of strong acids observed. With more reducing sediments, the picture is more complex because radiolytic oxygen may be involved in the partial breakdown of the organic component in the sediment. Here again though, it is likely that the thermal influence will greatly outweigh the influence of radiation. Finally, G values for hydrogen production were somewhat less than the optimal 0.45, hence use of this value provides a reasonable, but conservative estimate of radiolytic activity in actual systems.

TABLE 9

Gas Compositions and G values

T	Dose (Rads)	Mole Percent									Source
(°C)	(x 10^8)	H_2	O_2	N_2	CO_2	CH_4	CO	C_2H_6	$G(H_2)$	$G(O_2)$	
200	1.08	34.6	0.15	7.3	51.1	5.9	0.15	0.18	0.30		GME
200	0.60	25.1	0.12	14.8	55.4	3.9	0.14	0.41	0.20		GME
200	0	N.D.	0.20	15.5	84.3	TR	N.D.	N.D.	----		GME
25	0.60	57.2	0.55	29.2	13.0	N.D.	N.D.	N.D.	0.43		GME
200	0.64	36.7	0.13	9.58	55.3	0.17	0.15	N.D.	0.26		SNAP
200	0.60	47.5	0.19	8.23	43.5	0.46	0.14	N.D.	0.29		SNAP
200	0	1.07	0.49	15.4	83.1	N.D.	TR	N.D.	----		SNAP
25	1.09	19.2	19.7	60.4	0.70	N.D.	N.D.	N.D.	0.06		SNAP
200	1.43	70.4	0.15	9.87	17.8	1.30	0.48	N.D.	0.46		VEMA
150	0.33	37.8	11.5	43.2	7.5	N.D.	TR	N.D.	0.16	0.05	P.-Sm.
150	4.08	57.1	22.9	17.3	2.7	N.D.	TR	N.D.	0.09	0.04	P.-Sm.
150	0.33	56.9	0.5	32.4	7.5	N.D.	TR	N.D.	0.34	0.00	SeaH2O
150	4.08	55.4	15.7	26.0	2.9	N.D.	TR	N.D.	0.02	0.02	SeaH2O
127	100	66.4	30.4	2.5	0.1	N.D.	.03	N.D.	0.03	.013	P.-Sm.
127	100	59.2	27.5	12.1	1.1	N.D.	.02	N.D.	0.001	.0016	SeaH2O

TABLE 10

Comparison of Hydrogen G values With and Without a Head Space

	$G(H_2)$
1.7 cm^3 Head Space 2 g Seawater 0.64 x 10^8Rads	0.38
No Head Space 3.64 g Seawater 0.59 x 10^8 Rads	0.12

TABLE 11

Mass Balance Comparison Of Dissolved Ca, CO_2 and Missing O_2

Sediment Type	GME	GME	SNAP	SNAP	Vema
Dose Rate (KRad / Hr)	180	324	192	180	430
Moles CO_2 (x10^4) produced	1.2	1.3	1.2	.9	.3
Moles Ca (x10^4) produced	1.2	1.2	1.1	.9	.1
Moles O_2(x10^4) missing	.25	.41	.37	.45	.65

3.2 Synergistic Effects Involving Radiation and Temperature Gradients

To simulate the combined effects of near field temperature and radiation gradients, a far more elaborate apparatus was needed. This consisted of a titanium-lined autoclave with an internal diameter of 1.05 inches and an internal length of 30.6 inches. The autoclave had sample ports at either end so both hot and cool fluids could be obtained. It was also equipped with a 1.00 in O.D. titanium liner so that intact cores of sediment could be recovered at the end of a run. The autoclave plus heaters was enclosed in a stainless steel canister that allowed the system to be operated at the bottom of the pond in the LICA (Low Intensity Cobalt Array) facility. Dose rates within the autoclave are summarized in Table 12. One unfortunate feature of this arrangement was that to achieve parallel radiation and temperature gradients, it was necessary to operate with the heated end of the autoclave downward.

In comparing conditions expected around an actual waste canister with those in the autoclave it was found that the temperature gradient was appropriate, but that the radiation dose rate at the hot end was several orders of magnitude higher (assuming the penetrator design being considered by the U.S. program in late 1986). However, the gradient in radiation flux is appropriate, as would be expected since shielding in both cases is provided primarily by low Z elements. To summarize, whereas the time-temperature aspect of the experiment is in real time, radiation effects were much accelerated so that the dose received might mimic the total cumulative dose expected around an actual waste canister-penetrator package. In the event that bare canisters were emplaced, though, both the temperature and radiation fields would roughly approximate those existing during this experiment.

Two parallel experiments were done with this apparatus. Run 1 was done in the absence of radiation and lasted 41 days, while Run 2 was done in the LICA source and lasted 69 days (maximum dose 5×10^8 Rads). In both cases the temperature in the autoclave ranged from 300 to 40°C, while the pressure was maintained at 50 MPa. The sediment used in these experiments was a surficial brown clay from the floor of the mid-Pacific Ocean. It consisted primarily of illite, chlorite, quartz, and kaolinite (?), with enough organic material to completely reduce the iron in the sediment from the hottest part of the experiments. Thus in general, it was more reducing than "Sediment B", but appears to be quite similar to the sediment from the ISIMU experiment.

3.2.1 Mineralogic and Textural Observations

With regard to mineralogy, both experiments behaved as would be predicted from results presented earlier in this report. Only subtile changes in clay mineralogy were detectable, namely: some smectite formation and an improvement in the crystallinity of the illitic component of the sediment. Chlorite was not affected by the hydrothermal treatment. Smectite formation in the hot zone may account for the relatively high water content in the heated sediments at the bottom of the autoclave. In both experiments it was also found that the bottom 6 cm of core (T > 280°C) were compacted and had a bleached blue-gray color due to the reduction of iron by the organic material in the sediment. From 6 to 10 cm (280 - 260°C), the sediment was

brown but showed some evidence of bleaching. At 10 cm the color changed to a darker brown, which persisted to a distance of 25 cm from the bottom of the core barrel (260 - 160°C). Beyond this the brown color lightened slightly to that of normal unheated sediment, and at the top the sediment-seawater mixture remained fairly fluid.

3.2.2 Transport Processes and Inorganic Solution Chemistry

The following discussion will center first on the comparison between the on line samples obtained from the two experiments (Table 13), and then broaden to incorporate data obtained from post-test cores (Table 14). With regard to Table 14, it should be stressed that these pore fluids came from samples of quenched sediment that were also exposed to the atmosphere during autoclave disassembly. No attempt was made to analyze Fe, Mn, Si or Al, and it must be kept in mind that ion exchange reactions may have somewhat altered the concentrations of the other solutes. Probably the most striking difference between the two experiments is in the early samples from the hot end of the autoclave. Run 2 (with radiation) had much higher concentrations of sulfate, magnesium, boron, silicon, iron, and hydrogen ion. With pH, magnesium, and sulfate this trend persisted into the long term while boron, silicon, and iron concentrations in the two experiments were converging toward common values by the time the experiments ended. Less striking but also noteworthy, are the high silicon and manganese concentrations in both early and late samples from the cool end of Run 2. The silicon values, for example, are far in excess of quartz saturation but within the range of solubility measurements obtained using amorphous silica. In Run 1 (without radiation) the cool end silica concentrations were well below amorphous silica saturation and only slightly above that of quartz. A final, curious aspect of this data is that the 69-day samples from Run 2 had much smaller gradients in boron, manganese, magnesium, sodium, and chloride compared to what developed in Run 1 after only 41 days.

With regard to pore fluid chemistry (Table 14), both runs produced qualitatively similar concentration profiles. Sodium and chloride had obviously left the hot end in both cores, and in each there was an odd concentration maximum about half way down the core. Magnesium also exhibited a relative maximum toward the cool end, but superimposed on this was the very obvious depletion of magnesium due to clay-water interactions in the hot end of the autoclave. In contrast, calcium concentrations generally increased in samples taken from the hot end of the autoclave which probably reflect the redissolution of anhydrite. Potassium and boron are characteristically liberated during sediment-seawater interactions, and as expected, decrease toward the cool end. In comparing the two experiments, it is also evident that though Run 2 was longer, the concentration profiles are more poorly developed for sodium, chloride, magnesium, and potassium. Calcium on the other hand, was more strongly separated during Run 2. This correlates with a greater overall degree of magnesium depletion during Run 2, and higher potassium and boron concentrations. The simplest explanation for these differences, as well as for the unusual chemistry of the early samples from Run 2, is that mixing occurred during this experiment. This probably started during the emplacement of the assembly into the LICA source since the autoclave was already heated at this point and it proved necessary to tip the assembly on its side several times during this operation.

A second avenue of comparison is with the temperature gradient experiments done by Thornton and Seyfried (Table 13). Such comparisons are justified because, though Thornton and Seyfried used a shorter autoclave, the temperature gradient leading away from the hot end was roughly the same for both autoclaves. Further, similar sediments were used and the highest temperature in both experiments was the same (300°C). Surprisingly, the extent of transport was found to be quite different in the two suites of experiments (Table 15). Some of these differences, notably the behavior of magnesium, sulfate and calcium in Run 2, are explicable in terms of the mixing processes just discussed. Others, such as high ratios for boron and manganese and low ratio for iron, may reflect slight differences between the sediment. More perplexing is the behavior of elements such as potassium, silicon, sodium and chloride. One might imagine that, given all the similarities between the tests, at least these components would behave similarly. Yet, Runs 1 and 2 consistently show less transport, except where mixing was an obvious factor. This and the odd hump noted in the pore fluid concentration profiles suggest a need to quantitatively evaluate the influences of time and scale on the extent of transport.

The time dependent concentration profile of a "non-reactive" component (e.g. sodium chloride) was modeled by dividing the autoclave into 36 equal boxes with properties assigned to each based on temperature. Transport was then computed based on the concentration and temperature gradients between the two boxes and the average properties of the two boxes being considered at each step in the computation. The temperature dependence in the diffusion coefficient was approximated based on the Stokes - Einstein Equation (34) which, in turn, used viscosities for deionized water at 50 MPa (35). Diffusion coefficients ("D") in water were further modified to account for the presence of sediment based on the post-test water contents measured in the core. This was accomplished using the approximation that D (in sediment) = D (water)/F*P. It was further assumed that $F = P^{-n}$, where F is the formation factor, P the useful porosity (e.g. volume of interconnected water/volume of total sediment of), and n having an average value of 1.8 (36). It was also assumed that all the water in the sediment was interconnected, and that the sediment has an average grain density of 2.9. Parenthetically, it should be pointed out that this elaborate correction procedure proved to be superfluous since it produced essentially the same concentration profiles as when uncorrected diffusion coefficients appropriate to static water at temperature were employed. Soret coefficients for sodium chloride were estimated by drawing a smooth curve through the data of Caldwell (22) at low temperatures and assuming a value of 0.004 at 200°C (4, 21). Theoretical concentration profiles generated by this approach are illustrated for several cases in Figures 1-3. In the first case, a sharp temperature rise is assumed over the first three boxes at the hot end with the temperature then falling according to the actual temperature profile measured along the autoclave. In the second case, the hot end is essentially isothermal and the same temperature gradient as before was used in going from hot to cool end after the third box. For comparison, two types of analytic data are also depicted here. Open circles are chloride analyses from post test pore waters extracted from wet sediment. Crosses represent chloride values obtained by drying samples to obtain moisture content, and then resuspendging the dry sample in a known amount of water so that the total amount of chloride could be determined. Aside from a systematic

displacement, the two types of analytic data show essentially the same pattern, and the pattern is similar to that produced by the numerical model. The most obvious exception to this statement is that neither experiment developed a sharp minimum several inches in from the hot end, probably because pore fluids in this region were homogenized when samples were withdrawn immediately prior to terminating the experiments. In short, apparently much of the discrepancy between the two sets of experimental data can be ascribed to time and scale effects.

Such a model is also helpful in explaining why Thornton and Seyfried (21) obtained slightly different Soret coefficients when using an inert alumina matrix, in contrast to what was obtained when the autoclve was filled with marine clay. Putting dimensions and temperature gradients appropriate to their experiments into the program shows that this discrepancy probably arises because the system had not equilibrated in 32 days (Fig. 4). The model further suggests that had they used data from their 54 day samples (4) somewhat better agreement could be expected. A second interesting feature of the model is that it predicts a slight concentration maximum between the hot and cool ends of Runs 1 and 2. In the course of reducing data from the ISIMU experiment, the 70°C sample was excluded because it appeared high in most components and was presumed to be contaminated by the overlying body of seawater (though no obvious fracture system was found to explain how this fluid gained access to the sampler). An alternative explanation may be that, like maxima noted in Runs 1 and 2, this feature may be a relic of the non-steady state gradients that developed as the experiment approached equilibrium.

One final use of this model is to provide a baseline for interpreting the convective history of Run 2. By comparing the theoretical development of the chloride concentration profile with that actually found after the run, it follows that the pore fluid was truly static during only about the last third of the run. What probably happened in Run 2 was considerable convection of both sediment and seawater during the first few days of the experiment. Even a short exposure to such an environment might cause significant cracking of the organic component, and explain the immediate lowering of the pH. A record of unusual kerogen pyrolysis during Run 2 is also found in the concentrations of dissolved iron and manganese. In Run 1 the Fe:Mn ratio was about 0.4, while early in Run 2 a ratio of 2.3 was found. This, and the large concentration of dissolved iron (Table 13B) all support the contention that an unusual amount of organic matter was being broken down during the early part of Run 2. The other "fast" hydrothermal reactions noted in this report are the ion exchange reactions. Thus, it is not surprising that boron jumped immediately in Run 2 to values that were much above those in Run 1. The relatively short period when the entire mass convected was probably followed by a much longer period during which fluid moved through static sediment. Finally, judging from the chloride concentration profiles, during the last third of the test even this motion ceased. During this time only diffusion and the Soret effect acted to redistribute the various dissolved components in the pore fluid. To summarize, although Run 2 differed significantly from Run 1 this probably reflects the influence of convection, rather than significant differences arising from exposure to gamma radiation.

3.2.3 Organic Chemistry

As indicated earlier there is strong circumstantial evidence suggesting organic acids may be important reaction products when organic-rich marine are exposed to near-field conditions. These experiments verified this supposition. In addition to formic and acetic acid (Table 16), the chromatogram also indicated that small amounts of malonic, lactic, and propionic acids could be expected. No evidence (at a detection limit of about 0.0001 moles/liter) for the formation of oxalic, maleic, or benzoic acid was found. In the case of formic and acetic acids it was also found that they may reach high enough concentrations to influence solution pH and complex trace metals. Apparently, they may also persist for a long period of time. This behavior contrasts sharply with that of the more complex acids (e.g. malonic, lactic, and propionic acids), the concentrations of which were much diminished in the 69-day sample from Run 2. A final point concerns the relative influence of heat and radiation. Clearly, in spite of the age of the sample, the first entry in Table 16 demonstrates that heat rather than radiation is the principal agent causing formation of these compounds.

3.2.4 Radiation Effects

The major effect of radiation was, as with earlier experiments on kerogen containing sediments, production of radiolytic hydrogen along with lesser amounts of carbon dioxide, methane, oxygen, etc. (Table 17). By the end of the test hydrogen concentrations were about equal at both ends so it is possible to estimate the amount of hydrogen in the autoclave. By then comparing this with the dose received (Table 12) a bulk $G(H_2)$ of 1.0 was calculated for the system. The value is anomalously large, though Jenks (28) also found an unusually high value at the highest temperature he studied (to 0.8 between 170 and 180°C). Rather than a peculiar temperature effect, though, this number results from a combination of water radiolysis and the effects of radiation on kerogen at a temperature where thermal pyrolysis alone is quite effective. The cycling of excess sediment through the hottest part of the auoclave during the early part of Run 2 also probably played a role in generating this unusually high value.

TABLE 12

Dose Rate Inside The Autoclave
(inches from bottom of internal cavity)

Inches	KRad / Hour	Inches	KRad / Hour
0	295	18	1.15
2	214	20	.867
4	95.7	22	.621
6	45.4	24	.447
8	16.6	26	.331
10	7.38	28	.270
12	4.96	30	.214
14	2.73	32	.184
16	1.52	34	.2

TABLE 13A

Concentration of Major Elements in On Line Samples - PPT

Days/Temp.	Ca	Mg	K	Na	Cl	SO_4	pH
			Run 1 - No Radiation				
5 Hot	.52	.19	.86	12.3	21.4	-	5.9
5 Cool	.42	1.26	.52	10.8	20.8	-	7.0
13 Hot	.28	.15	.81	10.5	19.0	-	4.9
13 Cool	.43	1.26	.51	10.8	21.2	-	7.0
28 Hot	.43	.10	.77	9.9	17.2	-	4.9
28 Cool	.44	1.27	.53	11.1	20.4	-	6.7
41 Hot	.29	.12	.72	9.7	18.9	0.29	4.7
41 Cool	.47	1.41	.53	11.8	21.4	2.70	6.9
			Run 2 - With Gamma Radiation				
10 Hot	.17	.30	.86	11.8	21.6	0.74	3.6
10 Cool	.36	.96	.63	11.0	19.7	2.04	6.7
69 Hot	.11	.41	.67	10.8	19.1	0.49	3.2
69 Cool	.26	.67	.73	11.9	20.8	0.98	6.2

TABLE 13B

Concentrations of Trace Elements in On Line Samples - PPM

Days/Temp.	B	Mn	Si	Fe	Al	Br	Sr
			Run 1 - No Radiation				
5 Hot	21	251	429	93	1.6	-	5.9
5 Cool	6.7	9	25	1.8	.9	-	7.0
13 Hot	36	280	503	91	1.1	-	4.9
13 Cool	8.7	11	nd	nd	.9	-	7.0
28 Hot	34	200	400	45	.3	-	4.9
28 Cool	12	14	16	.1	.1	-	6.7
41 Hot	38	220	372	32	.5	-	4.7
41 Cool	17	22	21	.8	.5	-	6.9
			Run 2 - With Gamma Radiation				
10 Hot	91	170	800	390	.7	-	3.5
10 Cool	27	360	86	.5	.5	-	6.8
69 Hot	30	180	255	24	nd	76	3.1
69 Cool	31	210	82	2.3	nd	79	5.7

Elution times for fluoride, acetate and formate ions were found to be the same for the AS4 column used for inorganic anion analysis, consequently it was not possible to analyze these samples for fluoride. Neither nitrate or nitrite were detected.

TABLE 14

Concentrations of Post-Test Pore Waters
(Distance is cm from Hot End)

Length (cm)	Cl (PPT)	Br (PPM)	SO4 (PPT)	B (PPM)	Ca (PPT)	Mg (PPT)	Sr (PPM)	K (PPT)	Na (PPT)	% Water
				Run 1 - Without Gamma Radiation						
1	18.4	-	-	37	0.29	.12	9	.70	9.7	61.5
8	18.5	-	-	33	1.36	.25	21	.67	10.6	61.5
18	22.7	-	-	20	1.05	.90	17	.63	13.2	58.7
23	23.1	-	-	18	0.96	1.14	17	.57	13.6	60.2
25	22.8	-	-	21	0.85	1.24	14	.50	13.1	60.2
28	23.9	-	-	19	0.79	1.15	14	.53	13.5	61.3
33	25.4	-	-	25	0.61	1.19	10	.53	13.9	61.9
38	24.4	-	-	24	0.56	1.33	10	.53	14.1	62.9
44	23.7	-	-	20	0.55	1.41	11	.50	13.1	63.7
53	23.1	-	-	15	0.51	1.44	9	.50	12.5	74.6
66	20.9	-	-	16	0.42	1.22	8	.55	11.0	100
Length (cm)	Cl (PPT)	Br (PPM)	SO4 (PPT)	B (PPM)	Ca (PPT)	Mg (PPT)	Sr (PPM)	K (PPT)	Na (PPT)	% Water (#)
				Run 2 - With Gamma Radiation						
2	18.7	67	4.1	20	1.17	0.72	16	.70	11.7	60.5
7	20.0	70	4.2	18	1.23	0.73	14	.76	11.9	61.2
10	20.6	72	4.2	19	1.21	0.93	16	.70	12.2	60.2
13	20.8	71	4.5	16	1.30	0.77	8	.71	12.5	60.2
17	20.4	75	1.0	14	0.33	0.85	3	.67	11.9	60.1
19	20.7	78	0.77	14	0.32	0.83	1	.67	12.1	59.6
21	20.2	72	0.68	13	0.26	0.72	2	.73	12.1	58.7
23*	20.6	73	0.81	13	0.29	0.80	3	.68	11.9	58.1
36 (24)	20.8	76	0.71	14	0.29	0.78	2	.70	12.5	57.8
42 (30)	22.9	85	0.76	15	0.28	0.73	3	.69	13.2	56.8
44 (32)	21.7	77	0.77	16	0.26	0.87	4	.67	12.8	56.3
47 (35)	22.9	81	0.95	18	0.30	1.11	6	.75	13.3	57.6
49 (37)	22.0	78	1.01	19	0.33	1.16	5	.66	12.6	58.6
51 (39)	23.1	80	1.13	19	0.32	0.92	4	.70	13.4	59.6
54 (42)	22.0	77	1.09	20	0.27	1.10	4	.40	7.7	60.9
59 (47)	18.6	75	3.07	12	0.28	1.07	4	.58	9.5	62.9

* During extraction from the autoclave a 12 cm separation of the core occurred here, values in ( ) give actual position in the autoclave.
# % Water = 100 x (weight loss on drying)/(weight of wet sediment sample)

TABLE 15

Concentration Ratios Obtained During Temperature Gradient Experiments *

	Na	K	Ca	Mg	Si	SO4	Cl	Fe	Mn	B
				Run 1 / (Seyfried and Thornton)						
Hot End	1.3	1.5	3.0	0.7	0.9	1.3	1.6	0.3	2.8	4.0
Cool End	0.8	0.5	1.3	1.3	.04	1.1	0.9	--	0.2	1.8
				Run 2 / (Seyfried and Thornton)						
Hot End	1.5	1.4	1.1	2.4	0.6	2.3	1.6	0.3	2.3	3.2
Cool End	0.8	0.7	0.7	0.6	0.3	0.4	0.8	--	2.2	3.3

* Ratios refer to the last sample taken in each experiment. For example,after 54 days Seyfried and Thornton (Table 3) report 14.04 ppt Na from the cool end (100°C) of their sediment gradient experiment, and in Run 1 the final concentration in the cool end (41°C) was 11.8 ppt. Thus, the cool end entry for sodium in run 1 is 0.84, which rounds to 0.8.

TABLE 16

		Organic Acids Acetic Acid (M/L)	Formic Acid (M/L)
Run #1 - Hot	28 Days	.002	.001
Run #2 - Hot	10 Days	.001	.0003
Run #2 - Cool	10 Days	.0006	.0005
Run #2 - Hot	69 Days	.0005	.0003
Run #2 - Cool	69 Days	.0006	.0004

This sample was more than a year old at the time of analysis so the figures are of semiquantitative significance only.

TABLE 17

Gas Compositions from Run 2 After 69 Days

Mole %	H_2	O_2+ Ar	N_2	CH_4	CO	CO_2	C_2H_6
Cool End	11.0	16.8	70.7	0.25	nd	1.21	0.04
Hot End	75.6	2.13	6.59	1.09	nd	14.3	0.31
Moles/Kg x 1000	H_2	O_2+ Ar	N_2	CH_4	CO	CO_2*	C_2H_6
Cool End	79.0	121	506	1.79	nd	8.66	0.29
Hot End	67.7	1.91	5.9	0.97	nd	12.8	0.28

* An alternative estimate of the total dissolved carbon content was obtained by sampling both ends into preweighed amounts of sodium hydroxide solutions, and then running these solutions on a Corporation carbon dioxide analyzer. Results obtained in this manner were 7.9 and 17.6 millimoles total carbonate per kg for the cool and hot ends respectively.

4.0 PROGRAMMATIC APPLICATIONS

As stated in the introduction, one objective of this work was characterization of the near field environment in support of canister corrosion studies. In this vein one important finding is that at peak temperature the pore fluid becomes acidic in but a few days. Hydrogen ion concentrations on the order of 10^{-3} molar were observed so the corrosion resistance of penetrator and canister materials in acidified seawater must be verified. Using a pH of 3, however, is a conservative overtest since in every case where the heated sediment was coupled to a cooler body of sediment the pH ranged from slightly less acidic than this value to nearly neutral. In this regard, the ISIMU experiment was particularly important as it demonstrated that a continuous supply of magnesium to the heated region around a canister would, in fact, not cause the pH to plummet far below values obtained in isothermal closed system experiments. Instead acid generation is apparently slow enough that the buffer capacity of the seawater was not exhausted before the fluid returned to the cooler part of the experiment. Other environmental factors pertinent to corrosion processes were also evaluated. It was, for example, established that a range of oxygen fugacities could be expected based on sediment type, and that at the oxidizing end of this range even gold dissolves to the extent of several tens of parts per million in solution. This study also established that substantial amounts of certain transition metals, notably iron and manganese, may go into solution under certain conditions. When (or if) corrosion modeling evolves to the point that the effects of dissolved metals on corrosion rates can be evaluated, a supporting data base will already exist. In this context, this work also confirmed that any comprehensive corrosion program must evaluate the influence of organic acids and organic complexing agents, as well as the inorganic chemistry of the system.

A second class of concerns related to canister longevity was that of radiation effects. It appears, however, that these are not serious concerns. No evidence was found that radiolysis would produce high concentrations of aqueous oxidizing agents or large amounts of acid. Further, the G values obtained for hydrogen gas production greatly diminish the probability of a canister failing due to hydrogen embrittlement. About 200 ppm hydrogen can be absorbed before Ti Code 12 exhibits even the first indication of hydrogen embrittlement. The question then arises of how long it would take to produce enough radiolytic hydrogen to reach this level in a canister that is, for example, 1 cm thick. When such a calculation is performed (37), it turns out that all of the hydrogen produced in the first few centimeters around an unshielded canister would have to be absorbed immediately for between ten and twenty years if the metal is to reach the 200 ppm level. However, the uptake of hydrogen by titanium is a very slow process, so most radiolytic hydrogen will diffuse into the far field rather than be absorbed by the canister. If, in addition, a canister is shielded by the penetrator assembly the arguments against radiolytic hydrogen embrittlement become overwhelming. Thus, if hydrogen embrittlement is to occur to a significant degree it must involve the nonradiolytic dissociation of water (due to reduction by titanium from the canister or some other metal in the penetrator assembly). Finally, these experiments also provide a large body of empirical observations that bear witness to the general suitability of titanium-based canister materials. In every experiment cited the autoclave either contained titanium components or

was composed entirely of titanium or Ti Code 12. Yet, not one instance of titanium corrosion was observed. This applies to a variety of sediment types as well as the entire range of environmental conditions likely to be encountered in the subseabed disposal of nuclear waste. One general conclusion, then, is that a reasonable overall system model would assume the waste to be protected from hydrothermal leaching (except in the event of an accident) since there is every reason to believe that the canister could last at least a century.

Given the above conclusion it follows immediately that any coupling between near field effects and the integrity of the far field barrier must arise from the residual changes that persist after the thermal pulse has died away. If, for example, low density phases formed they might permanently displace a canister toward the sediment-seawater interface. Alternatively, such phases might migrate upward separately thus disrupting far field sediments above the canister. Using observed rates of hydrogen production, however, it is fairly easy to calculate that the near field would remain undersaturated with respect to hydrogen gas bubble nucleation by at least a factor of thirty (37). The other gas produced in appreciable quantities in these tests was carbon dioxide. At elevated temperatures the possibility exists of nucleating bubbles, while at lower temperatures clathrates might be anticipated. Taking carbon dioxide production from the GME sediments as an example, this amounted to about 1.3×10^{-4}moles of carbon dioxide in a system containing 0.15 moles of seawater (2.7 g). Thus, the mole fraction of carbon dioxide in the system was about 8.7×10^{-4}. At 500 bars this is considerably below that required for either bubble nucleation or clathrate formation (38, 39, 40). In fact, it appears that something like twenty times the carbon dioxide production noted in these experiments would be required before separate carbon dioxide rich phases could form (and this assessment assumes an essentially closed-system near field). A second category of long lasting changes are those involving the clay minerals present in the sediment. These experiments, though, demonstrated that these processes would only permanently affect those sediments lying within roughly the 50°C isotherm. Thus, a second conclusion of programmatic importance is that no mechanisms were identified in any of these studies whereby near field processes would degrade the integrity of the far field barrier.

Remaining, is the matter of clarifying the meaning of the term "near field". A variety of processes have been identified which may displace sediments from their "natural" state. In the hottest sediments anhydrite precipitates and magnesium-rich sheet silicates form from pre-existing clays. If the system remains relatively closed, this latter process will also lower pore fluid pH, thus facilitating dissolution of carbonates, zeolites or feldspars. In a relatively open system, or where the sediments contain sufficient carbonate to titrate the acid, the pH may remain nearly neutral. In this setting these minerals may, in fact, form rather than dissolve. If the sediments are rich in organic material, their pyrolysis may also play an important role in the pore fluid geochemistry. In addition to creating generally reducing conditions, pyrolysis may add carbon dioxide, methane and hydrogen (in addition to that produced by water radiolysis) to the pore fluids along with a wealth of organic acids able to further lower solution pH and complex metals. It was also found that, while all these processes proceeded vigorously at 300°C, they were much attenuated at 200°C. Thus, it

seems likely that most of the major mineralogic reactions involving silicate phases will lie within the maximum extent of the 125°C isotherm. At lower temperatures there are, however, other processes which will remove sediments from their "natural" state. Certainly, the pyrolysis of organic compounds may persist to as low as 70°C (41), though the rates are slower and the reaction products likely to be somewhat different. Probably of greater importance, though, is the fate of the high temperature reaction products which ride the temperature gradient outward. Among these may be considerable amounts of reduced iron and manganese. When precipitated, they may alter the sediment's sorptive properties and permeability. From the data presented it appears that most of the iron and manganese (as well as silica) will be deposited before reaching the fifty degree isotherm. Mass balance constraints also dictate that any acid reaching relatively cool sediments should also be neutralized by this point. Thus, as an approximation it seems reasonable to fix the outer boundary of the near field as the maximum extent of the 50° isotherm (e.g. at about 2 meters from the canister surface). Implicit in this designation is the stipulation that to qualify as a part of the "near field" the sediment must be displaced from its "natural" condition for a long period of time (e.g. longer than the expected life time of a canister). Nothing was found in this study which suggests that the subtle transient changes occurring in sediments heated but a few tens of degrees will, in the long term, affect their properties once the temperature returns to normal. Thus, eliminating these sediments from consideration greatly simplifies the definition of the near field without changing the analysis of overall system performance with regard to radionuclide migration.

Finally, it is important to stress the dominant role played by thermal processes as compared to radiation effects. If future work on near field sediment-seawater interactions is undertaken, one may safely eliminate radiation effects from the experimental matrix, or alternatively leave them until last when the systems are so well understood that relatively subtle departures from normal will be recognizable.

REFERENCES

1. Seyfried, W. E., P. C. Gordon, and F. W. Dickson, 1979, A new reaction cell for hydrothermal solution equipment, American Mineralogist, v. 64, p. 646-649.

2. Bischoff, J. L., and W. E. Seyfried, 1978, Hydrothermal Chemistry of Seawater from 25°C to 350°C, American Journal of Science, v. 278, p. 838 - 860.

3. Janecky, D. R. and W. E. Seyfried, 1983, The solubility of magnesium-hydroxide-sulfate-hydrate in seawater at elevated temperatures and pressures, American Journal of Science, v. 283, p. 831 - 860.

4. Thornton, E. C., 1983, Experimental and theoretical modeling of sediment-seawater hydrothermal interaction at constant temperature and in a thermal gradient: Implications for the diagenesis and metamorphism of marine clay and the subseabed disposal of nuclear waste. Ph.D. Thesis, Univ. Minnesota, 193 p.

5. Seyfried, W. E., E. C. Thornton and D. R. Janecky, 1981, Sediment-seawater interaction at elevated temperatures and pressures: Implications for the near field chemical environment, Subseabed Disposal Program Annual Report January to December 1979, Volume II - Appendices, SAND80-2577/II, Appendix E, p. 163 - 258.

6. Seyfried, W. E., and E. C. Thornton, 1981, Sediment-seawater interactions at 200 and 300°C, 500 bars Pressure: Chemical exchange and hydrothermal alterations, Subseabed Disposal Program Annual Report, January to December 1980, SAND81-1095/II, Volume II, Appendix E, p. 73-242.

7. Seyfried, W. E. and E. C. Thornton, 1981, Experimental and Theoretical Modeling of Hydrothermal Processes in the Near Field Environment, Appendix V, Subseabed Disposal Program Annual Report January to September 1981, v. 2, part 1, SAND82 - 0664, p. 717 - 806.

8. Thornton, E. C., and W. E. Seyfried, 1985, Sediment-seawater interaction at 200 and 300°C, 500 bars pressure: The role of sediment composition in diagenesis and low-grade metamorphism of marine clay, Geol. Society of America Bulletin, v. 96, p. 1287 - 1295.

9. Thornton, E. C., and W. E. Seyfried, 1987, Reactivity of organic-rich sediment in seawater at 350°C, 500 bars: Experimental and theoretical constraints and implications for the Guaymas Basin hydrothermal system, Geochimica et Cosmochimica Acta, v. 51, p. 1997 - 2010.

10. Surdam, R. C., S. W. Boese, and L. J. Crossey, 1984, The chemistry of secondary porosity, in Clastic Diagenesis, American Association of Petroleum Geologists Memoir: 37, p. 127 - 151.

11. Carothers, W. W., and Y. K. Kharaka, 1978, Aliphatic acid anions in oil-field waters - implications for origin of natural gas, American Association of Petroleum Geologists Bulletin, V. 62, p. 2441 - 2453.

12. Palmer, D. A., and S. E. Drummond, 1986, Thermal decarboxylation of acetate. Part I. The kinetics and mechanism of reaction in aqueous solution, Geochimica et Cosmochimica Acta, V. 50, p. 813 - 823.

13. Seyfried, W. E., and E. C. Thornton, 1984, Experimental studies of rock-water interaction processes in a thermal gradient: Thermal diffusion and sediment-seawater interaction in the near field-environment, Appendix B, Subseabed Disposal Program Chemical Response Studies Annual Report October 1981 through September 1982, L.H. Brush, ed., SAND82 - 2713, p. 25 - 194.

14. Manheim, F. T., and F. L. Sayles, 1974, Composition and origin of interstitial waters of marine sediments, based on deep sea drill cores, C. 16, The Sea, Volume 5: Marine Chemistry, E.D. Goldberg, ed., John Wiley and Sons., p. 527 - 569

15. Geldermalsen, L. A., and J. W. Wegereef, 1985, The influence of temperature on migration of radionuclides in deep-sea sediment: Simulation experiments concerning sorption and heat flow related to deep-sea disposal of high-level radioactive waste, Final Report 1981-1984, Dutch Ministry of Economic Affairs.

16. Goldberg, S., and R. A. Glaubig, 1986, Boron absorption and silicon release by the clay minerals kaolinite, montmorillonite, and illite, Soil Sci. Soc. Am. J., v. 50, p. 1442 - 1448.

17. Cronan, D. S., 1974, Authigenic minerals in deep-sea sediments, C. 15, The Sea, Volume 5: Marine Chemistry, E.D. Goldberg, ed., John Wiley and Sons., p. 491 - 526.

18. Baes, C. F. and R. E. Mesmer, 1976, The hydrolysis of cations, Johy Wiley and Sons, 489 p.

19. Decarreau, A., 1985, Partitioning of davalent transition elements between octahedral sheets of trioctahedral smectites and water, Geochimica et Cosmochimica Acta, v. 49, p. 1537 - 1544.

20. Giordano, T. H., 1985, A preliminary evaluation of organic ligands and metal-organic complexing in Mississippi Valley-type ore solutions, Economic Geology, v. 80, p. 96 - 106.

21. Thornton, E. C., and W. E. Seyfried, 1983, Thermodiffusional transport in pelagic clay: Implications for nuclear waste disposal in geologic media, Science, v. 220, p. 1156 - 1158.

22. Caldwell, D. R., and S. A. Eide, 1981, Soret coefficients and isothermal diffusivity of aqueous solutions of five principal salt constituents of seawater, Deep-Sea Research, Ser. A, v. 28, p. 1605 - 1618.

23. Seyfried W. E., E. C. Thornton, F. L. Sayles, 1985, Heat-transfer experiment in marine pelagic clay: Implication for subseabed disposal of high-level radioactive waste and contact metamorphism in the Guymas Basin, Gulf of California, Chemical Geology, v. 53, p. 135 - 153.

24. Gundlach, H. and W. Thormann, 1960, Versuch einer deutung der Entstehung von Wolfram and Zinnlegerstatten, Zeitschr. Deut. Geol. Gesell., v. 112(I), p. 1 - 35.

25. Kazanskii, L. P., E. A. Torchenkova, and V. I. Spitsyn, 1974, Structural principals in the chemistry of heteropolycompounds, Russian Chemical Reviews, v. 43, p. 525 - 538.

26. Rimstidt, J. D. and H. L. Barnes, 1980, The kinetics of silica-water reactions, Geochimica Cosmochimica Acta, v. 44, 1683 - 1699.

27. Kennedy , G. C., 1950, A portion of the system silica-water, Economic Geology, v. 45, p. 629 - 653.

28. Jenks, G. H., and J. R. Walton, 1981, Radiation chemistry of salt-mine brines and hydrates, ORNL-5726, 72 p.

29. Jenks, G. H., 1975, Gamma-radiation effects in geologic formations of interest in waste disposal: A review and analysis of available information and suggestions for additional experimentation, ORNL-TM 4827, p. 1 - 26.

30. Krumhansl, J. L., 1986, Observations regarding the stability of bentonite backfill in a high-level waste (HLW) repository in rock salt, SAND83-1293, 98 p.

31. Spitsyn, V. I., B. D. Balukova, and M. K. Savushkina, 1981, Influence of irradiation with gamma-quanta and beam of accelerated electrons on the sorption parameters of clay minerals of the montmorillonite group, The Scientific Basis for Waste Management, IV, Stephen V. Topp, ed., p 703 - 707.

32. Glass, R. S., 1981, Effects of radiation on the chemical environment surrounding waste canisters in proposed repository sites and possible effects on the corrosion process, SAND81-1677, 96 p.

33. Thomas, J. K., 1969, Elementary processes and reactions in the radiolysis of water, Advances in Radiation Chemistry, v. 1, p. 103 - 192.

34. R. A. Horne, 1972, Water and Aqueous Solutions, Wiley-Interscience, C.5, p. 175 - 244.

35. Kestin, J., and H. Dipippo, 1972, Table 2r-8 Viscosity of compressed water and superheated steam, in American Institute of Physics handbook, Gray, D. E., ed., McGraw-Hill, Inc., p. 2-246 - 2-247.

36. Berner, R. A., 1880, Early diagenesis a theoretical approach, Princeton University Press, C. 5, p. 15 - 55.

37. Krumhansl, J. L., 1984, Radiation Effects in the Near Field, Appendix C, Subseabed Disposal Program Chemical Response Studies Annual Report October 1981 through September 1982, L.H. Brush, ed., SAND82 - 2713, p. 195 - 229.

38. Wiebe, R., and V. L. Gaddy, 1939, The Solubility in Water of Carbon Dioxide at 50°, 75° and 100°C at pressures to 700 atm., Am. Chem. Soc. Jour., v. 61, p. 315 - 318.

39. Wiebe, R., and V. L. Gaddy, 1940, The Solubility of Carbon Dioxide in Water at Various temperatures from 12 to 40°C, Am. Chem. Soc. Jour., v. 62, p. 815 - 817.

40. Collins, P. L. F., 1979, Gas Hydrates in CO_2 bearing Fluid Inclusions and the Use of Freezing Data for Estimation of Salinity, Economic Geology, v. 74, p. 1435 - 1444.

41. Hunt, J. M., 1979, Petroleum geochemistry and geology, W. H. Freeman and Company, C. 4, p. 69 - 149.

FIGURES

Fig. 1 Top: Distribution of sediments (left) and seawater (right) in autoclaves during Runs 1 and 2.

Bottom: Comparison of thermal profiles during Runs 1 and 2 (solid lines) with that used in Soret transport modeling (dotted).

Fig. 2 Comparison of modeled concentration profiles (solid lines) with pore water concentration profiles during Run 1. Concentrations are represented as the ratio of chloride content at some point following the run to that in the initial pore fluid. The heavier solid line represents a model with a uniform 300°C temperature at the bottom, while the lighter solid line models a setting with a peak temperture of 300°C slightly in from the end of the autoclave and a temperature of 260°C at the bottom of the autoclave. Circles are analyses performed on pore fluid squeezed out of the sediment while the triangles are analyses based on bulk water content and bulk chloride of the sediment.

Fig. 3 Comparison of modeled concentration profiles (solid lines) with pore water concentration profiles from Run 2. The same symbols were used as in Fig. 2.

Fig. 4 Comparison of modeled enrichment due to soret transport with that observed by Seyfried and Thornton (21). The comparison is expressed as the natural log of the hot end concentration divided by that in the cool end at various times.

Fig. 5 Ion chromatograms for two sets of samples from Run 2 showing the relative abundances of organic acids in these samples at two times.

Fig. 6 Phase diagram for clathrates as a function of mole fraction carbon dioxide and temperature. Note that experimental concentrations do not approach the level necessary for nucleation of a seperate carbon dioxide rich phase.

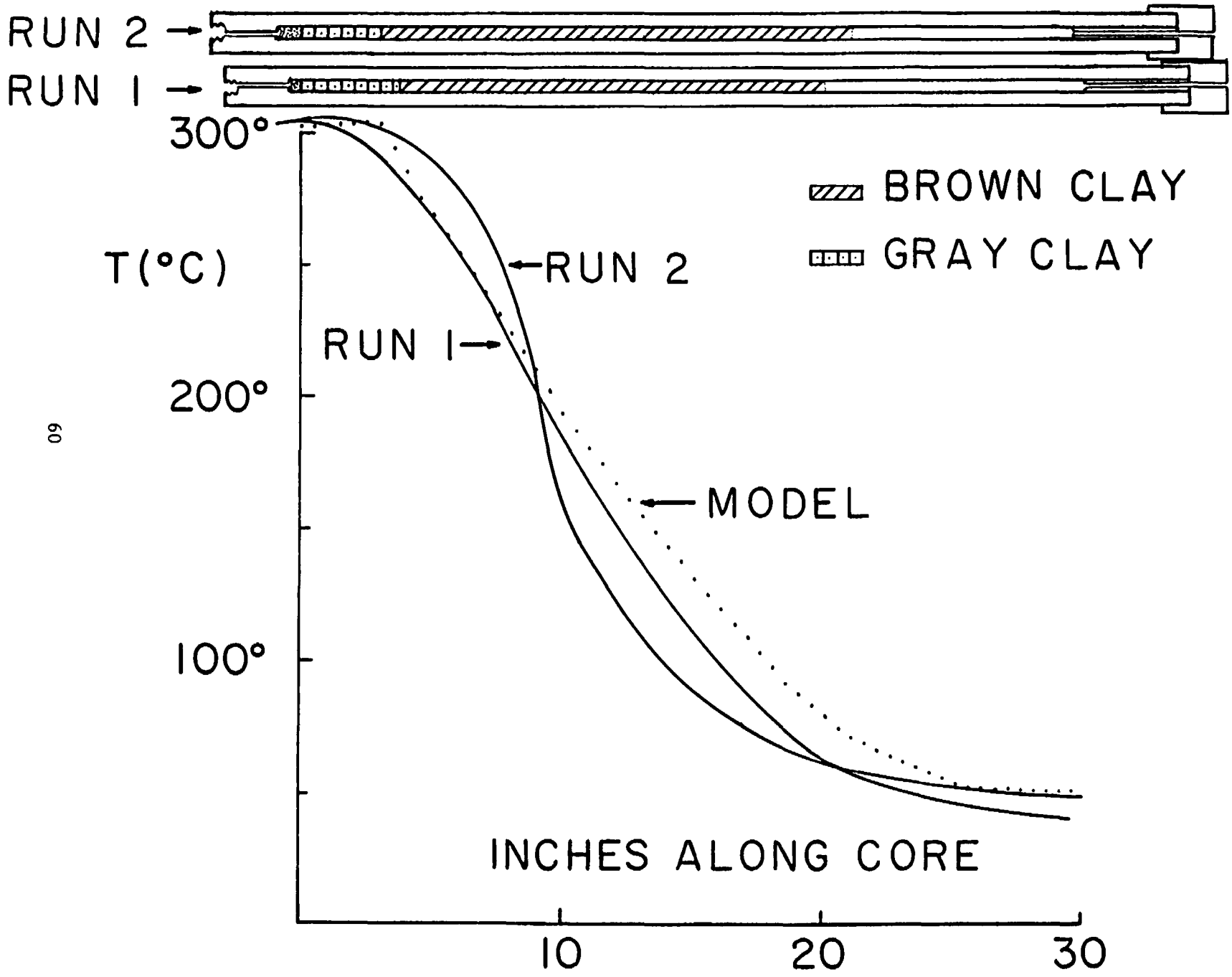
RUN 2
RUN 1
BROWN CLAY
GRAY CLAY
300°
200°
100°
T(°C)
RUN 2
RUN 1
MODEL
INCHES ALONG CORE
10
20
30

Fig. 1

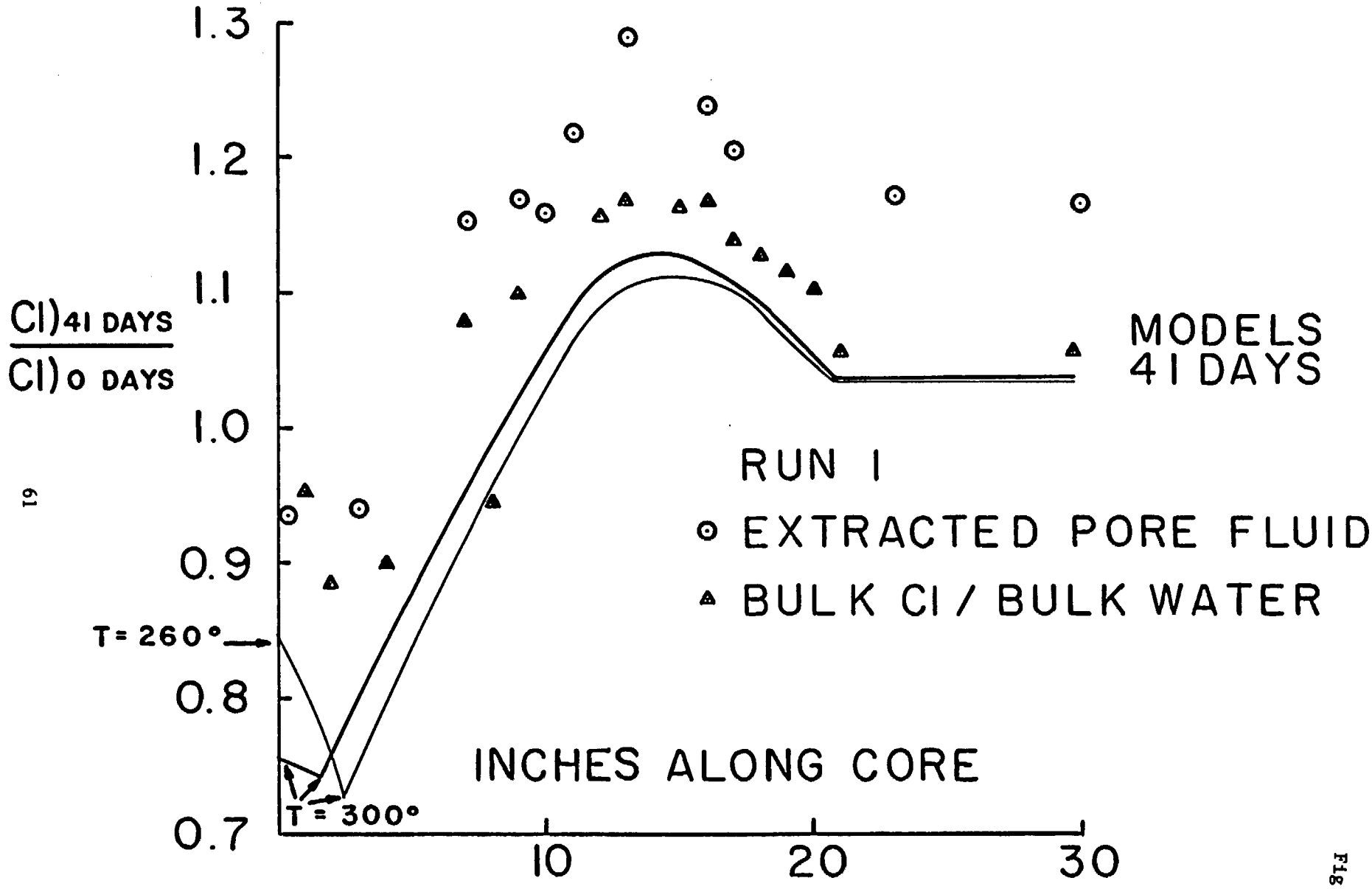
1.3
1.2
1.1
1.0
0.9
0.8
0.7
Cl)41 DAYS / Cl)0 DAYS
T= 260°
T = 300°
10
20
30
INCHES ALONG CORE
MODELS 41 DAYS
RUN I
EXTRACTED PORE FLUID
BULK Cl / BULK WATER

Fig. 2

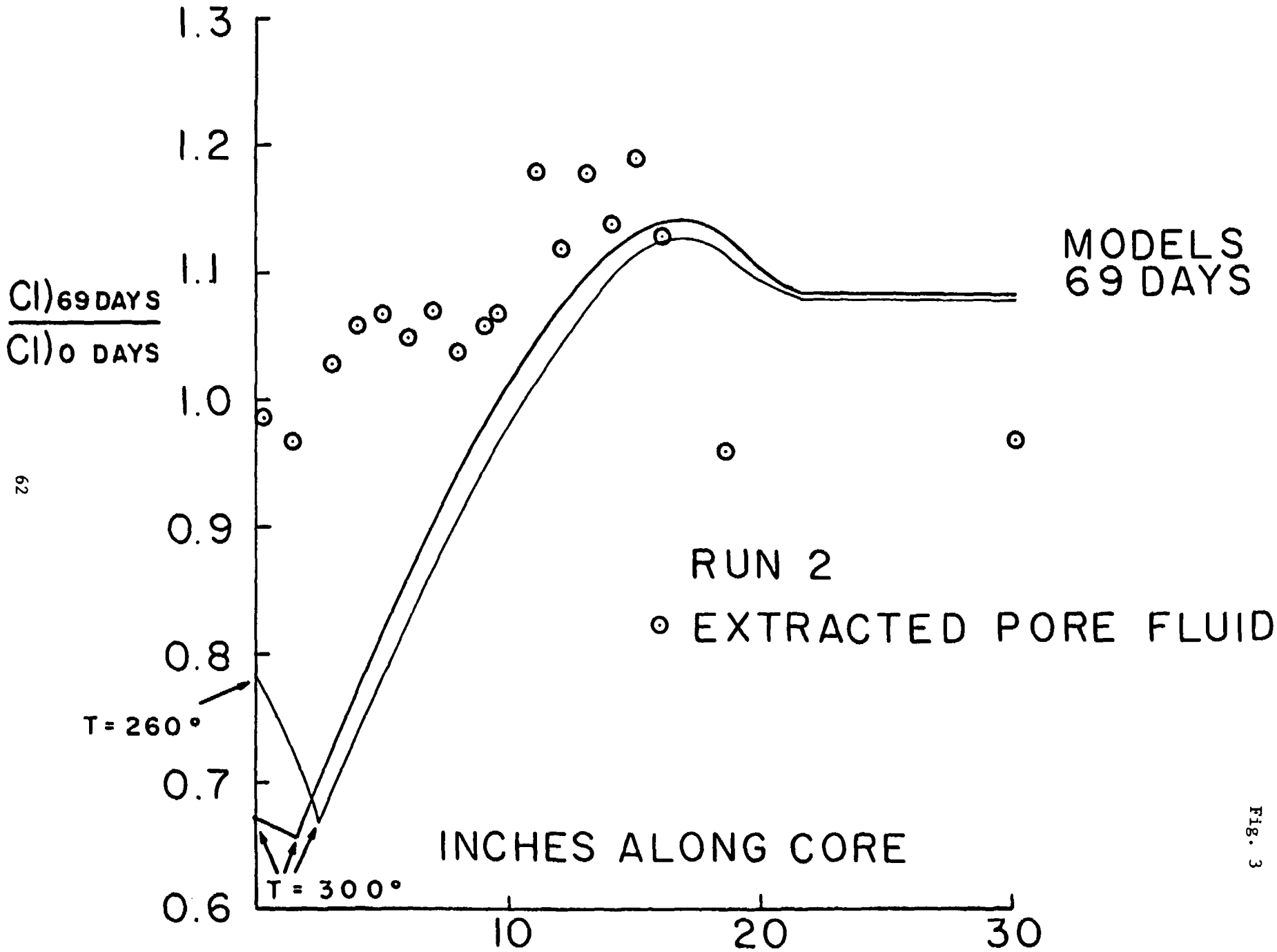
1.3
1.2
1.1
1.0
0.9
0.8
0.7
0.6
Cl)69 DAYS / Cl)0 DAYS
MODELS
69 DAYS
RUN 2
EXTRACTED PORE FLUID
T = 260°
T = 300°
INCHES ALONG CORE
10
20
30

Fig. 3

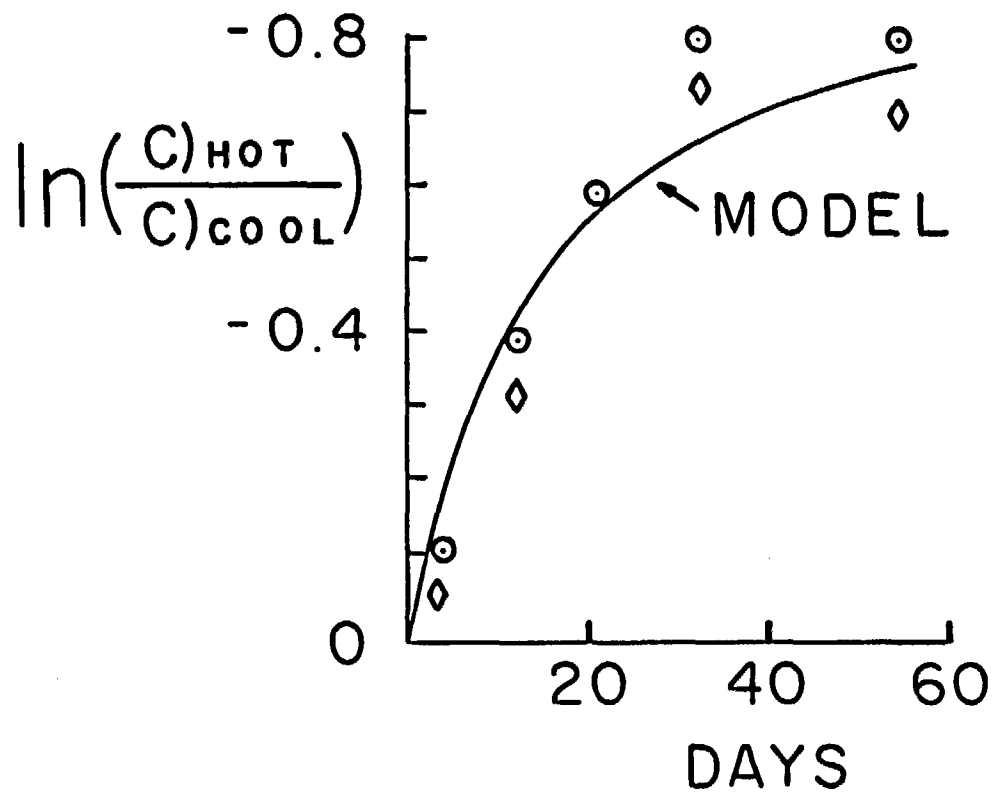

⊙ CHLORIDE
◊ SODIUM
} From: Thornton and Seyfried, 1983

Fig. 4

State University of New York
at Stony Brook
Marine Sciences Research
Center
Attn: J. K. Cochran
Stony Brook, NY 11794

State Univesity of Utrecht
Institute of Earth Sciences
Department of Geochemistry
Attn: G. de Lange
Budapestlaan 4
3508 TA Utrecht
NETHERLANDS

University of Minnesota
Department of Geology and
Geophysics
Attn: W. E. Seyfried, Jr.
Minneapolis, MN 55455

Universite de Neuchatel
Lab Geologie
Attn: F. Nyffeler
11, rue Emile Argand
CH-2000 Neuchatel
SWITZERLAND

University of Rhode Island
Graduate School of
Oceanography
Attn: K. R. Hinga
S. Ferry Rd.
Narragansett, RI 02883

University of Washington
College of Ocean and Fishery
Sciences
Attn: G. R. Heath
Seattle, WA 98195

U.S. Environmental Protection
Agency
Attn: R. Dyer
J. Neiheisel
M. Varela
401 M. St. SW
Washington, DC 20460

Woods Hole Oceanographic
Institution
Department of Chemistry
Attn: F. L. Sayles
Woods Hole, MA 02543

Woods Hole Oceanographic
Institution
Department of Geology
Attn: C. D. Hollister
Woods Hole, MA 02543

Internal Distribution:

1512	K. L. Erickson
1846	B. C. Bunker
3141	S. A. Landenberger (5)
3151	W. I. Klein (3) for DOE/TIC
3154-1	C. L. Ward (8) for DOE/OSTI
5248	B. T. Kenna
6230	W. C. Luth
6233	T. M. Gerlach
6233	J. L. Krumhansl (5)
6300	R. W. Lynch
6330	W. D. Weart
6331	M. D. Siegel
6334	D. R. Anderson
6334	S. G. Bertram-Howery
6334	L. H. Brush
6334	L. S. Gomez
6312	R. D. Klett
6334	M. G. Marietta
6334	A. K. Rutledge
8524	J. A. Wackerly

SPECIAL
FOURTH CLASS

KNOXVILLE
JUN 19 '89
TENN

SPECIAL MAIL
POSTAGE
FOR PRIVATE USE $300
0.90
METER
504316

Sandia National Laboratories

Rec'd by
Name
Bldg.
Org.
Rec'd by

VOID VOID VOID VOID
VOID VOID VOID VOID
VOID VOID VOID VOID
VOID VOID VOID VOID
VOID VOID VOID VOID

POSTAGE AND FEES PAID
DEPARTMENT OF ENERGY
DOE-350
U.S. MAIL

United States Department of Energy
Office of Scientific and Technical Information
Post Office Box 62
Oak Ridge, Tennessee 37831

OFFICIAL BUSINESS
PENALTY FOR PRIVATE USE, $300

3925 FS- 1 B
US NUCLEAR REGULATORY COMMISSION
ATTN DIRECTOR
OFFICE OF NUCLEAR MATERIALS AND SS
WASHINGTON, DC 20555